

Compact Photostorage Systems: New Materials and Designs for Integrated Energy Harvesting and Storage

Original

Compact Photostorage Systems: New Materials and Designs for Integrated Energy Harvesting and Storage / Mirone, Alice; Cartabia, Luca; Martin, Irene; Rubino, Andrea; Kriegel, Ilka; Gatti, Teresa. - In: SOLAR RRL. - ISSN 2367-198X. - 10:1(2026), pp. 1-23. [10.1002/solr.202500926]

Availability:

This version is available at: 11583/3006448 since: 2026-01-10T17:06:02Z

Publisher:

Wiley

Published

DOI:10.1002/solr.202500926

Terms of use:

This article is made available under terms and conditions as specified in the corresponding bibliographic description in the repository

Publisher copyright

(Article begins on next page)

REVIEW OPEN ACCESS

Compact Photostorage Systems: New Materials and Designs for Integrated Energy Harvesting and Storage

 Alice Mirone¹ | Luca Cartabia² | Irene Martin¹ | Andrea Rubino¹ | Ilka Kriegel¹  | Teresa Gatti^{1,2} 
¹Department of Applied Science and Technology, Politecnico di Torino, Torino, Italy | ²Center for Materials Research, Justus Liebig University, Giessen, Germany

Correspondence: Ilka Kriegel (ilka.kriegel@polito.it) | Teresa Gatti (teresa.gatti@polito.it)

Received: 14 November 2025 | **Revised:** 14 December 2025 | **Accepted:** 15 December 2025

Keywords: direct light energy storage | photobattery | photocapacitor | photostorage device | sustainable energy

ABSTRACT

The growing demand for flexible and autonomous electronics has accelerated the development of compact energy systems capable of both harvesting and storing solar energy. Photobatteries and photocapacitors represent a new generation of self-charging devices that merge photovoltaic and electrochemical functions within a single structure. These systems overcome the conversion losses and bulkiness of conventional solar-battery combinations, enabling miniaturized, efficient, and sustainable power sources. This review summarizes recent progress in materials, architectures, and design strategies for compact photostorage systems. This work will focus, in particular, on two-terminal (2T) monolithic configurations that provide the highest integration level. Advances in inorganic semiconductors such as transition-metal oxides, sulfides, and lead-free perovskites, as well as organic materials including conductive polymers, dyes, and carbon nanostructures, have greatly enhanced photo-charge generation, mobility, and retention. Furthermore, innovations in gel and solid-state electrolytes have improved flexibility, safety, and long-term stability. Despite significant progress, major challenges remain in mitigating charge recombination, optimizing energy density and standardizing performance evaluation. By integrating recent results and emerging trends, this review outlines key directions for the rational design of next-generation self-powered photostorage systems that could underpin the future of portable, wearable, and sustainable energy technologies.

1 | Introduction

The global transition toward decentralized and self-sustained energy systems has accelerated the exploration for technologies that can efficiently capture, convert, and store renewable energy at small scales. The exponential growth of wearable electronics, portable sensors, environmental monitoring tools, and the Internet of Things (IoT) has intensified the need for lightweight, flexible, and autonomous power sources capable of continuous operation without high maintenance [1–3]. Traditional energy setups, in which solar cells are externally coupled to batteries or supercapacitors, suffer from conversion losses, voltage mismatches, and bulky architectures, which limit their integration into portable or flexible devices [4, 5].

To overcome these issues, compact photostorage devices, which consolidate both light-harvesting and energy-storage functions

in a single unit, have emerged as a promising new generation of self-powered systems [6–9]. Such hybrid devices directly convert sunlight into stored electrical energy, combining the photo-conversion function of solar cells with the electrochemical storage capability of batteries or supercapacitors, thereby reducing energy loss and simplifying device architecture [10, 11]. By merging both functions, compact photostorage systems exhibit improved round-trip efficiency, mechanical integration, and design flexibility [12].

Two main device classes have been identified: photobatteries (PBs) and photocapacitors (PCs), sometimes referred to as photo-supercapacitors (PSCs) [1, 3, 8]. In PBs, the photogenerated electrons and holes drive redox reactions at the electrodes, leading to high energy densities (E_d) but slower charge-discharge kinetics. In contrast, PCs store charge electrostatically at the electrode/electrolyte interface, yielding high power densities (P_d), rapid

This is an open access article under the terms of the [Creative Commons Attribution](https://creativecommons.org/licenses/by/4.0/) License, which permits use, distribution and reproduction in any medium, provided the original work is properly cited.

© 2026 The Author(s). *Solar RRL* published by Wiley-VCH GmbH.

response, and long cycle life, albeit at lower energy density [2, 4, 13–15]. These complementary characteristics make both systems relevant for different applications, from micro-power storage to continuous low-energy operation.

From a design standpoint, device configuration plays a crucial role in determining overall performance. As reported in previous studies [6, 8, 16, 17], three major configurations are distinguished: four-terminal (4T), three-terminal (3T) and two-terminal (2T). While 4T and 3T architectures allow independent optimization of photovoltaic and storage components, they also suffer from larger interfacial energy losses and more complex wiring. Conversely, 2T monolithic designs achieve the most compact and efficient integration, combining both functionalities into a single photoactive electrode pair and significantly reducing energy dissipation [14, 18]. As a result, 2T systems are now at the center of research on flexible, wearable, and transparent self-charging power units [19, 20].

Recent advances in photoactive materials have been decisive in improving these integrated systems. Transition-metal oxides (TMOs) such as TiO_2 , WO_3 , and V_2O_5 are among the most studied materials due to their tunable band structures, high stability, and semiconducting properties [21–27]. Similarly, metal sulfides like NiCo_2S_4 and MoS_2 exhibit enhanced redox activity and charge–transfer efficiency, especially when coupled with oxides or carbon nanostructures [25, 28–31]. Lead-free halide perovskites, such as $\text{Cs}_2\text{NaBiI}_6$, $\text{Cu}_3\text{Bi}_2\text{I}_9$, and $\text{Ag}_{0.5}\text{Cs}_{0.5}\text{Bi}_3\text{I}_{10}$, have recently emerged as environmentally friendly alternatives with remarkable light-absorption and charge-transport properties [24, 32, 33]. On the organic side, carbon-based materials, conductive polymers, and organic dyes are being widely explored for their flexibility, low weight, and tunable optoelectronic behavior [2, 34–45]. The combination of these materials into hybrid or heterojunction electrodes often leads to improved charge separation, reduced recombination, and enhanced specific capacitance (C_s) [28, 29, 46, 47].

In addition to electrode development, electrolyte engineering is a major driver of performance improvements. The transition from liquid to gel-polymer or solid-state electrolytes enhances mechanical stability, safety, and compatibility with flexible substrates [27, 36, 48–50]. Innovative photo-responsive electrolytes, such as 2-nitrobenzaldehyde-based systems, can even participate in the light-driven charge-storage process, offering an elegant route toward fully self-rechargeable supercapacitors [34].

Despite this progress, important challenges remain. The close proximity of photoactive and storage layers in 2T devices increases the probability of charge recombination, while interfacial resistance and energy-level misalignment still limit charge–transfer efficiency [18–27, 51–55]. Furthermore, the absence of standardized testing protocols for evaluating parameters such as photoconversion efficiency (PCE), C_s , and energy or power density complicates direct comparison between proposed systems [56, 57]. Achieving a unified framework for performance assessment is therefore essential to accelerate technological transfer and device optimization [58, 59].

This review provides an updated overview of the materials, architectures, and performance metrics that define today's compact photostorage devices research. Special attention is devoted to 2T integrated devices, inorganic–organic hybrid materials and emerging trends in electrolytes and flexible substrates. By

mapping current advances and outlining persistent limitations, this work highlights the pathways toward efficient, miniaturized, and sustainable solar-powered energy-storage systems, capable of meeting the rising energy demands of portable and wearable technologies [5, 9, 58, 59].

2 | Theoretical Foundations

Energy storage plays a crucial role in the efficient utilization of solar energy conversion. In this context, two main classes of energy storage devices can be distinguished: batteries and capacitors (or supercapacitors) [1]. These systems rely on fundamentally different energy storage mechanisms, which strongly influence their electrical characteristics and potential applications.

Conventional capacitors store energy electrostatically, enabling high power densities while offering limited energy densities. In contrast, batteries store energy chemically, providing high energy densities at the expense of lower power densities [2, 3]. Supercapacitors combine several attractive features, including power densities comparable to those of standard capacitors, short charging times, and excellent cycling stability, while maintaining E_d higher than conventional capacitors [2, 4]. Due to these complementary characteristics, batteries and supercapacitors serve different yet synergistic roles in energy storage applications. Continuous research efforts are directed toward enhancing their performance in order to bridging the gap between high energy and high-power operation. Such developments are expected to expand the practical applicability of supercapacitors, which currently remain a relatively emerging and developing technology.

From an application standpoint, batteries are particularly suited for systems requiring sustained energy supply, whereas supercapacitors excel in rapid charge–discharge scenarios and high-power pulses, making them ideal for small-scale or transient-load devices. Depending on these operational distinctions, the integration of solar energy conversion systems with either of these storage technologies offers diverse design strategies and performance outcomes [1, 5]. Nonetheless, achieving efficient coupling between a photo-conversion unit and the chosen energy storage component demands careful materials selection, interface engineering, and system optimization to ensure both stability and energy transfer efficiency.

2.1 | Device Designs

The integration of energy conversion systems with energy storage units can be achieved through a variety of architectural configurations [6] and by employing different types of devices [7, 8]. For what concern the PV component, in particular, energy storage elements have been successfully coupled with dye-sensitized solar cells (DSSCs) [9], perovskite solar cells (PSCs) [10, 11], and organic solar cells (OSCs) [8, 60]. Such integration aims to combine solar energy harvesting and on-site energy storage within a single, compact system.

As illustrated schematically in Figure 1a–c, three main device architectures have been proposed to achieve this multifunctional integration, both in PBs and PCs:

- *Four-terminal (4T) configuration* (Figure 1a): In this design, the energy conversion unit and the energy storage device

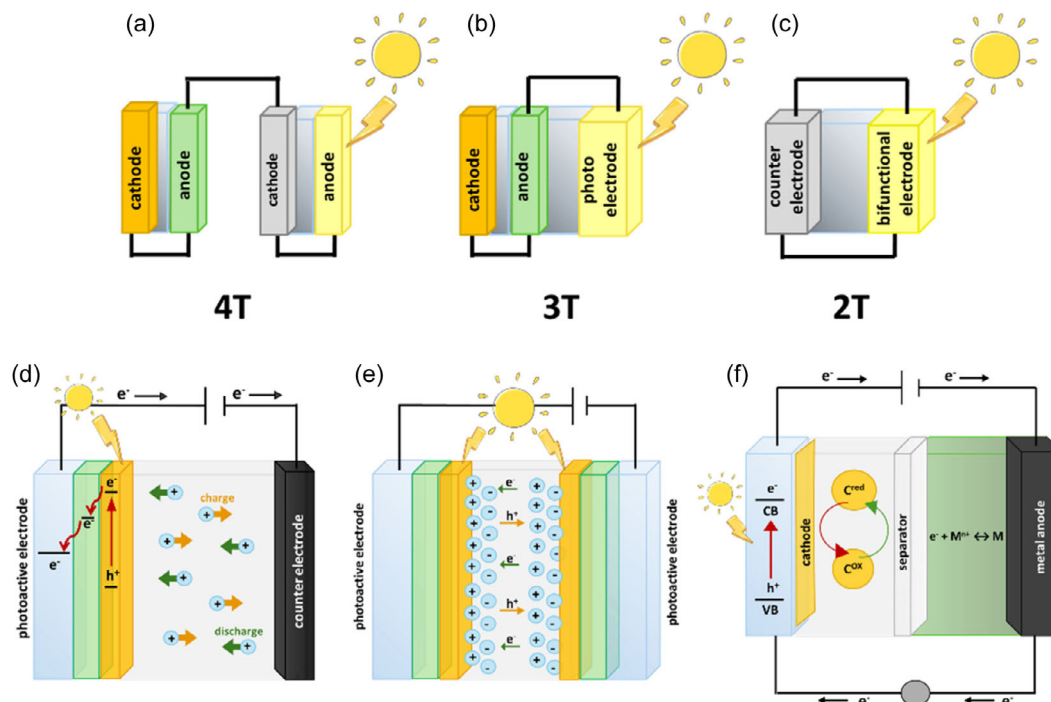


FIGURE 1 | Schematic representation of (a) 4T, (b) 3T, and (c) 2T integrated devices and schematic mechanisms of (d) asymmetric PC, (e) symmetric PC, and (f) PB.

are connected externally through a conventional electrical circuit. The two subsystems remain physically and functionally distinct, allowing great flexibility in combining different photovoltaic and storage technologies. Since the interconnection relies on simple cabling, this configuration does not require complex interface engineering and can accommodate a broad range of material systems.

- **Three-terminal (3T) configuration** (Figure 1b): Here, the conversion and storage units share a common electrode, which simultaneously participates in both functionalities. For instance, DSSCs have been coupled to capacitive electrodes that exhibit good electrochemical compatibility with the photoelectrode materials. This architecture represents a semi-integrated system, enabling closer interaction between the photovoltaic and storage components while maintaining partial structural independence.
- **Two-terminal (2T) configuration** (Figure 1c): The most compact and fully integrated design consists of only two electrodes. Typically, one functions as the photoactive electrode for light-to-electricity conversion, while the other serves as the energy storage electrode. In certain cases, symmetric configurations have been reported, in which both electrodes combine photoactive and capacitive properties. In this design, the boundaries between energy conversion and storage are effectively eliminated, resulting in an actual integrated photo-rechargeable system [8, 13].

Four- and three-electrode systems suffer from several intrinsic limitations [14]. Their complex geometries and multiple external connections lead to increased energy losses and, consequently, lower storage efficiency [3]. In addition, these architectures require a careful engineering of the electrical circuit to properly

integrate the energy conversion and storage units. The 2T configuration has emerged as a promising alternative to address these issues. Its compact architecture enables the simultaneous realization of both photovoltaic and storage functions within a single integrated device. This multifunctionality makes the 2T approach particularly appealing for the development of wearable and portable photo-rechargeable systems.

Nevertheless, engineering such a device requires optimization of numerous interdependent parameters, including the selection of suitable photoactive materials, efficient charge-transport media (electrolyte), and complementary counter-electrode or support materials. Each component plays a critical role in determining the overall electrochemical response and long-term performance of the integrated system.

2.2 | Energy Conversion and Storage Mechanisms

Since batteries and supercapacitors rely on fundamentally different energy-storage mechanisms, their photo-rechargeable counterparts also operate according to distinct working principles (Figure 1d-f) [15]. Both can generally be described as two-electrode devices that integrate light harvesting, charge generation, and storage within a single architecture [16]. The first photo-supercapacitor (PSC) was introduced by Miyasaka and Murakami in 2004 [1]. Their device consisted of a TiO_2 photoelectrode coupled with an organic dye, a carbon-based counter electrode exhibiting capacitive behavior and an ionic electrolyte. Upon illumination, the dye absorbed photons and generated electron-hole pairs. Electrons were injected into the TiO_2 conduction band and then transferred to the activated carbon electrode, while holes remained in the dye molecules. The high surface area and porosity of the carbon material enabled efficient charge accumulation, allowing the device to

perform rapid charge and discharge cycles typical of supercapacitors, reaching a C_s of 0.69 F cm^{-2} , in 1 h of photocharging.

In general, the working process of a PC/PSC includes three main stages: (i) light conversion (photon absorption and photocharge separation) within the photoactive layer, (ii) migration of charge carriers through their respective transport pathways, and (iii) charge accumulation at the capacitive electrode, with the formation of an electric double layer (EDL), which (iv) finally can release the stored energy like conventional supercapacitors (Figure 1d,e) [17].

In contrast, PBs, despite a similar photo-induced charge separation process as a first step, store energy through faradaic redox reactions rather than electrostatic accumulation. In these systems, the main stages are the following: (i) photogeneration of charges, (ii) the photogenerated electrons migrate toward the metal anode leading to the metal reduction, while the photogenerated holes are responsible of the species oxidation at the cathode; finally, (iii) the stored energy can be released through the inverse redox process, following the same working principle as traditional rechargeable batteries (Figure 1f) [17].

While these general mechanisms describe the operation of PCs/PSCs and PBs, practical implementations often vary due to differences in device engineering, material selection, and interfacial design. In particular, PCs/PSCs architectures are commonly categorized as symmetric or asymmetric, depending on whether both electrodes are composed of same or different materials and functionalities. Such variations strongly influence charge separation, transport, and overall energy-storage performance. At last, additional charge storage mechanism can arise in PCs and PSCs from highly reversible redox reactions typically localized at the electrode surface, giving rise to devices presenting pseudocapacitive or hybrid storage mechanisms.

2.3 | Challenges and Limitations

Despite more than twenty years since the first prototype, 2T photo-rechargeable systems are still at an early development stage, mainly due to several intrinsic limitations. One major issue is charge recombination, which arises from the short distance between electrodes in compact configurations. This can be mitigated through careful electrolyte selection or by introducing efficient charge-transport layers that promote carrier separation.

A further challenge lies in the dual role of certain materials, which often perform well in either energy conversion or storage, but not both simultaneously. Achieving a suitable balance therefore requires precise material pairing and interface design. Additionally, the 2T configuration typically suffers from higher internal resistance caused by complex interfacial processes within multifunctional layers, leading to lower charge-discharge potentials and reduced overall efficiency [18]. These constraints explain why most integrated photo-rechargeable studies so far have focused on 3T systems. Device and material engineering are thus required to overcome these limitations and optimize the performances of new-generation 2T devices.

3 | Materials

In view of developing light-driven energy storage devices, a wide range of materials presents compelling properties as colloidal

solution of nanoparticles (NPs). In particular, doped transition metal oxides as indium tin oxide (ITO) [61, 62], iron-doped zinc oxide (IZO) [63], fluorine-indium doped cadmium oxide (FICO) [64], niobium-doped titanium oxide (Nb-doped TiO_2) [65], and strontium titanate (SrTiO_3) [66] nanocrystals (NCs) solutions have shown charge storage properties under illumination, as a consequence of photodoping [67]. Photo-chargeable nanomaterials in dispersion differ substantially from those used for other dark reactions because their function relies on the light-driven accumulation, stabilization, and controlled release of charges within a fluid environment. In dispersions, the solvent, surface ligands, and dynamic colloidal interactions play an essential role in enabling long-lived charge separation, buffering local redox changes, and preventing premature recombination [68]. These features make dispersed nanomaterials highly adaptable platforms for studying fundamental photocharging mechanisms, as well as for tuning charge density and release kinetics through chemical control of the medium. As one significant example, Brozek et al. reported IZO NCs with an areal capacitance of $33 \mu\text{F/cm}^2$, corresponding to 233 F per unit of NC volume. Other inorganic compounds presenting energy-storage properties related to photo- and electro-chromism and on-demand photocatalysis are colloidal solutions of metal sulfides as CdS_2 [69], Ti-based metal organic frameworks (MOFs) [70], and organofunctionalized polyoxometalates (POMs) [71, 72]. Remarkable activity for delayed solar hydrogen evolution reaction and dye degradation have been also reported for organic materials, i.e., dye-sensitized carbon nitrides (CNx) slurries [73] and poly(heptazine imide) salts [74]. As a result, these compounds represent potential candidates as photoactive and energy storage layers in PB and PC. Nevertheless, the charge storage properties of the previously mentioned colloidal solutions might not directly translate when the same materials are deposited in thin film form. In fact, the transition from liquid to solid state is accompanied by a change in the dielectric of the NCs' surrounding environment, leading to a variation of the optoelectronic properties of the material [75, 76]. The deposition of NCs on a substrate may also lead to the formation of inhomogeneous or cracked film, enhancing scattering phenomena and consequent charge losses [76]. Thus, when integrated into photo-chargeable devices, these same nanomaterials must transition from freely diffusing colloids to architectures that permit efficient light absorption, scalable charge storage, and mechanical or electrochemical stability. Devices often require immobilization, percolation networks, or hybrid solid-liquid configurations to mediate electron extraction and minimize charge losses. In contrast, nanomaterials used for traditional dark reactions operate without the need for prior photocharging and instead rely on intrinsic catalytic pathways or surface redox processes that proceed directly under reaction conditions [77, 78]. As a result, while dark-reaction catalysts prioritize sustained turnover and robustness, photo-chargeable dispersed nanomaterials must balance illumination-driven charge accumulation, colloidal stability, and compatibility with device interfaces—making their design challenges and operational constraints fundamentally distinct [79]. For this reason, efficient coupling of light harvesting and charge storage is commonly achieved via combination of layers of different materials, each one contributing with a single functionality to the overall performance of the device. These compounds are hereby introduced and discussed, focusing on their implementation in both PB

and PC as energy storage, charge transport and light absorbing layers.

3.1 | Inorganic Materials

A wide range of materials exhibit promising properties for photo-rechargeable applications, which can broadly be classified into inorganic and organic categories. These two groups display distinct behaviors, primarily due to their different physicochemical characteristics. Inorganic materials are typically investigated in the form of nanostructures, such as nanocrystals, since the nanoscale enhances charge accumulation and improves electrochemical performance. They are usually semiconductors with well-defined bandgaps, and their intrinsic properties can be tuned to modulate the optical and electronic behavior of the resulting electrodes and, consequently, of the overall device [19, 20]. Notably, inorganic compounds such as metal oxides, metal sulfides, and perovskites are often combined with organic

materials during electrode engineering to exploit their complementary advantages. Such hybrid architectures can balance mechanical flexibility, light absorption, and charge-transport efficiency, leading to improved device functionality [51, 52]. Representative examples of inorganic materials employed in 2T PBs and PCs/PSCs are shown in Figure 2 and discussed later in the text.

3.1.1 | Metal Oxides

Among the various materials investigated for light energy harvesting and storage, transition metal oxides (TMOs) represent one of the most extensively studied classes due to their semiconducting behavior, structural versatility, and chemical stability [80]. TMOs can exist in multiple crystalline phases and morphologies, each influencing their electrochemical and optical properties. Both the synthesis route and deposition technique critically determine the resulting performance. In particular, nanoscale TMOs, such as nanoparticles (NPs), are of great interest since

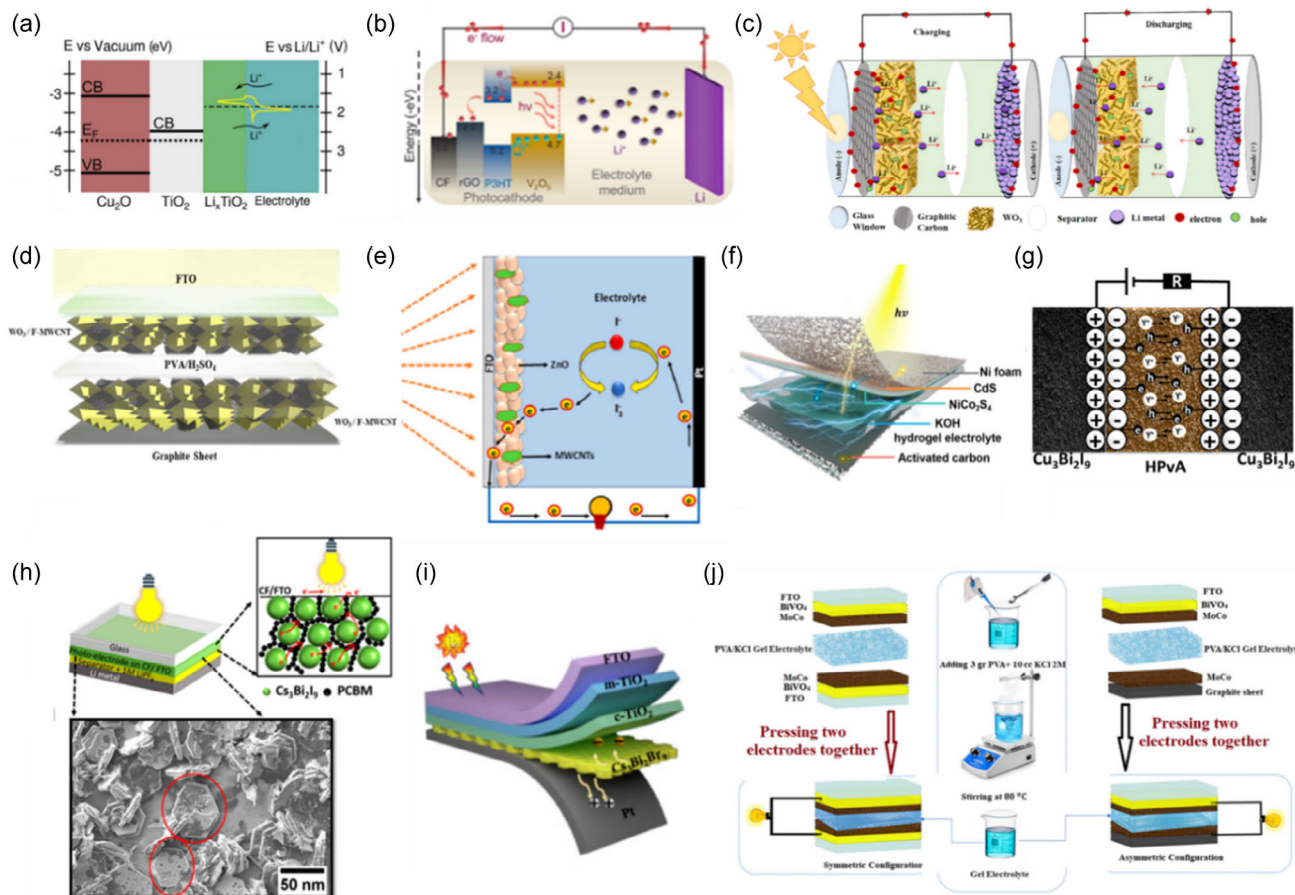


FIGURE 2 | Schematic representation of some 2T photo-rechargeable devices based on inorganic materials: (a) Li-ion PB based on $\text{Cu}_2\text{O}/\text{TiO}_2$ photocathode. Reproduced under the terms of CC-BY 4.0 license [22], Copyright 2021, American Chemical Society. (b) Li-ion PB based on V_2O_5 photoelectrode: Reproduced under the terms of CC-BY 4.0 license [21], Copyright 2023, Wiley. (c) Charging and discharging mechanism of Li-ion PB based on WO_3 photoanode. Reproduced with permission [23], Copyright 2025, Wiley. (d) Asymmetric PSC based on $\text{WO}_3/\text{MWCNTs}$ dual-function electrodes. Reproduced with permission [27], Copyright 2025, Elsevier. (e) Zn-ion PSC based on ZnO NPs on MWCNTs photoactive electrode. Reproduced with permission [54], Copyright 2024 Elsevier. (f) Flexible PSC based on CdS/ NiCo_2S_4 heterojunction as photoelectrode. Reproduced with permission [25], Copyright 2025, Elsevier. (g) Symmetric PSC based on lead-free inorganic perovskite as dual-functional electrodes. Reproduced with permission [24], Copyright 2023, Elsevier. (h) Li-ion PB based on lead-free perovskite photoactive electrode. Reproduced with permission [53], Copyright 2021, American Chemical Society. (i) all-solid-state PB based on lead-free perovskite photoactive material. Reproduced with permission [55], Copyright 2024, Elsevier. (j) Symmetric and asymmetric PSC based on MoCo/ BiVO_4 composite photoactive material. Reproduced with permission [26], Copyright 2025, Elsevier.

their high surface area enhances electrochemical activity, leading to improved energy and power densities [81]. Interestingly, TMOs NPs with controlled size and morphology can be obtained adopting cost-effective synthetic approaches, such as liquid phase synthesis (LPS) protocols (sol–gel, hydro/solvothermal synthesis, electrodeposition) [82, 83], with a low economic and environmental impact on the preparation of the active layer. TMOs are widely employed as electrode materials for energy storage because of their intrinsically high theoretical specific capacitance (C_s) and their ability to form composites with carbon-based materials, which further enhance conductivity and stability [84]. Among them, titanium dioxide (TiO_2) stands out as one of the most representative and extensively investigated materials for both energy conversion and storage applications. It is widely employed as the electron-conductive and mesoporous component in DSSCs [85–87], where its structural and electronic properties make it ideal for efficient charge transport [88, 89]. Recent studies have focused on doping TiO_2 with elements such as nickel [90, 91], magnesium [92], and other transition metals to enhance light absorption, improve charge separation, and ultimately increase the power conversion efficiency. TiO_2 -based DSSCs have also been successfully integrated into photo-rechargeable devices, where TiO_2 serves as the photoanode, enabling the coupling of light-harvesting and energy-storage functionalities within a single architecture [7, 9, 93, 94]. Ciria-Ramos et al. investigated a $\text{TiO}_2/\text{Cu}_2\text{O}$ photocathode in a lithium photobattery (Figure 2a), where Cu_2O acted as the light-harvesting material and TiO_2 as the capacitive element, resulting in fast charge times and a conversion efficiency of 0.29% [22]. Another example is vanadium pentoxide (V_2O_5), which has been employed as a photoactive electrode in lithium-ion PBs, as reported by De Volder and coworkers (Figure 2b) [21]. Their system achieved a PCE of 0.22% under one-sun illumination. The same group also utilized V_2O_5 as the light-harvesting component in a zinc-ion PC, demonstrating its versatility across different electrochemical configurations [95]. Furthermore, Banerjee et al. employed vanadium-doped iron oxide nanoflowers as photoactive materials in aqueous PCs, where doping extended the absorption window and improved both the C_s and the long-term stability of Fe_2O_3 [96].

Building on the use of TMOs as photoactive materials in PBs, Sajjad et al. recently employed tungsten trioxide (WO_3) as a photoanode, achieving high capacity and a PCE of up to 6% in a 2T configuration operating over a wide voltage range (Figure 2c) [23]. In another study, Momeni et al. combined WO_3 with multi-walled carbon nanotubes (MWCNTs) to enhance the capacitive response in an asymmetric 2TPC (Figure 2d), confirming the suitability of WO_3 for integrated energy devices [27]. The use of tungsten-based materials further reflects the growing research focus on abundant, environmentally benign transition metals for sustainable photo-rechargeable systems.

Another representative example of this trend is manganese oxide (MnO_2). Yildirim and Daş investigated its electrical behavior by comparing pure MnO_2 and MnO_2 /graphene-based devices, showing that the hybrid system exhibited superior performance as a photodiode in a self-powered device [97]. Similarly, Vanalakar et al. demonstrated that MnO_2 , when used as a conductive material for supercapacitors, exhibited a notable

photoresponse under illumination, leading to the design of a promising self-chargeable device [98].

Zinc oxide (ZnO) also represents a versatile and widely investigated photoactive material for energy-storage applications, both in its pristine and doped forms [99–101]. Owing to its favorable electronic structure and tunable morphology, ZnO has been employed as a light-active electrode material in PCs and PSCs [102]. As with other TMOs, its properties can be further improved through compositional modification. For instance, Eswaramoorthy et al. incorporated MWCNTs into ZnO to enhance its electrical conductivity in a flexible PC (Figure 2e) [54]. Sankir et al. reported ZnO nanoflakes grown on reduced graphene oxide (rGO), showing that 16% rGO significantly enhanced the photo-charging and storage capabilities of the oxide in a 2T PSC device [103]. Likewise, Saini et al. developed a PSC based on ZnO nanoparticles doped with MWCNTs, demonstrating excellent capacitance retention (C_R) and long-term stability over repeated cycles [104].

Overall, these studies demonstrate the crucial role of TMOs, including TiO_2 , V_2O_5 , Fe_2O_3 , WO_3 , MnO_2 , and ZnO , in advancing photo-rechargeable device research. Their structural versatility, chemical stability, and tunable electronic properties make them key components for achieving efficient, durable, and environmentally sustainable 2T energy-conversion and storage systems. The ability to tailor their composition, morphology, and interfaces continues to drive progress toward next-generation integrated photorechargeable technologies.

3.1.2 | Metal Sulfides

Following the extensive study of TMOs, metal sulfides (MSs) have recently gained attention as promising alternatives for integrated photorechargeable systems, owing to their high electrical conductivity, multiple oxidation states, and strong redox activity. Despite the wide use of TiO_2 in photo-conversion processes, its sulfide analog, titanium disulfide (TiS_2), remains comparatively underexplored. Narayanan et al. reported TiS_2 as a photoactive material for self-rechargeable Li-ion PBs, showing a higher lithium-binding energy than TiO_2 and improved charge-storage behavior. In their system, $\text{TiS}_2/\text{TiO}_2$ nanosheets cathodes suggested that the coexistence of oxide and sulfide phases can further enhance device performance [105]. Recent literature indicates that MSs are often combined with oxides [28, 29] or used as binary systems due to their high redox activity, efficient electron transport, and abundance of active sites [25, 31, 30]. Li et al. developed a 2T PSC using a $\text{CdS}/\text{NiCo}_2\text{S}_4$ heterojunction photocathode (Figure 2f), combining the photoactive properties of cadmium sulfide (CdS) with the pseudocapacitive response of NiCo_2S_4 , achieving promising energy and power densities, though efficiency values were not reported [25]. Nickel- and cobalt-based sulfides have also been widely explored: Lu et al. studied NiCo_2S_4 in both aqueous flow and sodium-ion PBs, reporting moderate performance and limited cycling stability, suggesting the need of further optimization [30]. More recently, Najafi et al. electrodeposited a ternary MnNiCoS layer on TiO_2 nanotubes, achieving an efficient photoactive electrode with excellent photosensitivity and C_s [31]. This work underlines the synergistic advantages of combining MSs with TMOs, leveraging their complementary optical and electrochemical

properties to enhance the performance of integrated 2T photo-rechargeable devices.

Altogether, by coupling strong redox activity with excellent charge transport, MSs offer a powerful route toward high-performance and durable 2T photorechargeable devices.

3.1.3 | Lead-Free Inorganic Perovskites and Perovskite-Inspired Materials

All-inorganic halide perovskites (ABX_3 -type structures) have attracted tremendous interest for photo-conversion applications owing to their exceptional optoelectronic properties [32]. While they are primarily employed in photovoltaics [106–108], recent studies have extended their use to integrated systems capable of both light harvesting and energy storage. Popoola et al. reported a lead-free inorganic halide perovskite-inspired material (PIM), $Cu_3Bi_2I_9$, used in a symmetric PSC incorporating a gel electrolyte (Figure 2g). The device exhibited enhanced C_s under illumination and excellent C_R [24]. The shift toward lead-free perovskites and PIMs is largely driven by safety concerns related to Pb leaching in liquid electrolytes and by the superior environmental safety of lead-free alternatives compared with their Pb-based counterparts. Accordingly, an increasing number of studies are focusing on these low toxicity compositions [109]. Chesta et al. demonstrated the potential of a $Ag_{0.5}Cs_{0.5}Bi_3I_{10}$ photocathode in aqueous zinc-ion PBs, achieving high stability and good performance, confirming the viability of such PIMs for future photo-rechargeable devices [33]. Lead-free perovskites and PIMs have also been explored in lithium-ion PBs. Tewari et al. employed a 3D Cs_2NaBiI_6 PIM as both the photoactive and energy-storage material, achieving promising rate capability, cycling stability, and improved overall performance compared with their earlier design (Figure 2a) [53, 110]. Similarly, cesium-bismuth-based PIMs have garnered significant interest: Li et al. used $Cs_3Bi_2Br_9$ as the photoactive component in a 2T all-solid-state PB (Figure 2i), revealing that redox processes involving bismuth play a central role in device operation. Interestingly, they further demonstrated that multiple cells could be connected in series to enhance total output performance [55].

Overall, lead-free inorganic perovskites and related PIMs combine strong photoactivity, stability, and safety, positioning them as promising materials for next-generation 2T photorechargeable devices.

3.1.4 | Composite Materials

To achieve dual-function operation in photorechargeable systems, compact devices are often designed by combining two or more materials through heterojunction engineering. A representative example is the work of Ramadi et al., in which the authors integrated $FeCo_2O_4$ nanoflowers with Bi_2S_3 nanorods to form a photoactive electrode for a 3T zinc-ion PSC. The device exhibited excellent cycling stability and C_R [46]. Within the same class of zinc-ion PSCs, Li et al. developed a two-terminal (2T) device featuring a $MoS_2/NaTaO_3$ heterostructure deposited on carbon felt, achieving a significant enhancement in capacitance under illumination and demonstrating a promising configuration for photochargeable systems [47]. Other studies have also employed molybdenum disulfide (MoS_2) in hybrid devices, although most examples involve coupling DSSCs with conventional supercapacitors in 4T architectures [111]. An additional innovative zinc-ion

PSC was reported by Liu et al., who utilized carbon-coated CdS on ZnO nanorods as a composite photocathode material, achieving high stability with minimal loss of C_s [29]. Similarly, Momeni et al. developed a 2T PSC combining manganese sulfide (MnS) with a $V_2O_5/BiVO_4$ photoanode, which delivered enhanced C_s , higher P_d , and improved stability compared to bare vanadium oxide composites, attributed to superior light absorption and faster charge transfer [28]. In a related study, Momeni, Renani, and coworkers reported a molybdenum-cobalt sulfide (Mo-Co-S) coupled with bismuth vanadate ($BiVO_4$) for use in PSCs, comparing symmetric and asymmetric 2T configurations (Figure 2j). Both systems showed good performance, but the asymmetric design exhibited higher power and E_d , confirming its superior suitability for direct light-energy storage applications [26]. Even if both the systems presented good properties, the asymmetric device showed higher power and E_d , indicating the best suitability of this configuration for direct light-energy storage applications. TMOs and MSs are often coupled to reach outstanding properties, as in the work of Kajana et al., in which is presented a Ag_2CrO_4/SnS photoanode for PC device [112]. They obtained a promising C_s and demonstrated a good stability after 50 cycles of cyclic voltammetry. In contrast to PSCs, PBs incorporating composite materials remain relatively rare. Cui et al. presented a 2T PB featuring a $LiFePO_4/TiO_2$ composite photocathode paired with a Li-ion anode, which showed increased capacity under illumination and improved overall performance compared to conventional $LiFePO_4$ cathodes, highlighting the potential of composite architectures to enhance both energy conversion and storage properties [113].

Collectively, composite and heterostructured designs offer a powerful strategy to boost efficiency and stability in compact 2T photo-rechargeable technologies.

3.2 | Organic Materials

As shown in the previous chapters, PSCs and PBs are complex systems that often require careful engineering and material-choice in order to optimize both the light harvesting and the energy storage. The rapid expansion of the Internet of Things (IoT) and the growing demand for portable and wearable sensors also call for devices that could power such tools while being compact, flexible, and lightweight at the same time. In this context, organic materials are crucial to combine efficiency requirements with cost-effectiveness and versatility. Therefore, this vast class of materials with unique and tunable structural and electronic properties has been raising a large wave of interest in the field of compact PCs and PBs. Organic materials gained particular success to produce PSCs thanks to their implementation in several compartments of the final device. Dyes are commonly employed in the photovoltaic (PV) unit of both PCs and PBs, while conductive polymers and graphitic carbonaceous materials are usually ideal (super)capacitive materials. There are also examples of organic electrolytes (see Section 5), which represent an intriguing but challenging alternative to the more common water-based ones. This section, instead, presents a brief and general overview of the most recent developments of compact PB and especially PC/PSC architectures that feature organic materials. These are divided into three macro classes, according to their chemical nature: carbon nanomaterials, dyes, and photosensitive organic molecules and conductive polymers. The discussion focusses on

their use for 2T PCs/PSCs, as it is the main field of application, but some of the most recent development of organic materials for PBs are also listed.

3.2.1 | Carbon Nanomaterials

3.2.1.1 | Nanocarbons. Nanocarbons are a broad class of organic materials that comprise a wide range of structures, among which are activated carbon (AC) and porous carbon. They have been extensively used as electrode materials in the energy storage unit PSCs, thanks to the low cost, high specific surface area, and conductivity [114]. These properties make them ideal candidates for supercapacitors, achieving high power output energies and allowing fast charge–discharge rates. In particular, the great specific surface areas that characterize these materials radically boost the capacitive charge storage by adsorption of the ions at the electrode–electrolyte interface (electrical-double-layer capacitors, EDLCs) [115]. In PBs, nanocarbons are mainly chosen as electrode materials and flexible substrates, but their use as conductive additives and charge stabilizers is also rapidly growing [116]. The fabrication of hybrids by combining nanocarbons with conductive polymer or metal oxides is also able to radically increase the pseudocapacitive behavior, thus leading to greater E_d [117, 118]. Activated carbon and porous carbon were the first materials to achieve commercial success for the production of electrodes for EDLCs. AC is obtained by physical or chemical activation processes that enhance the porosity, specific surface area, and conductivity. The materials are easily fabricated starting from cheap and available sources like coal, wood, or even bio-wastes, which are heated at temperatures between 400°C and 800°C in the presence of KOH, H_3PO_4 , or $ZnCl_2$ (chemical activation) or treated between 800°C and 1000°C in flow of CO_2 , air, or steam (physical activation). The result is a porous structure with high cycle stability, chemical resistance, and surface areas up to 3000 $m^2 g^{-1}$ [119, 120]. Templating approaches are also frequently adopted in the synthesis of porous nanocarbons in order to specifically tailor the porosity and thus control the electrode behavior [121, 122]. The first example of AC use in a PC dates back to the pioneering work of Miyasaka et al., who combined a dye-sensitized solar cell (DSSC) with an activated-carbon-based SCs in a two-electrode setup, which represents the first example of a charge-storage device powered by solar light [1]. This supercapacitor achieved a specific capacitance of 0.69 $F cm^{-2}$, but the same research group was able to reach a fivefold higher energy output with a three-electrode setup also using AC [123]. Lately, Bhaumik et al. reported a new 2T organic PSCs (Figure 3a), where activated charcoal served as eco-friendly and cost-effective active electrode material and 2-nitrobenzaldehyde as electrolyte [34]. The authors demonstrated the non-ionic 2-nitrobenzaldehyde undergoes photo-induced transformation into benzoic acid derivatives and transient ionic species that act as electrolyte. The final device displayed a high specific capacitance of 90 $F g^{-1} cm^{-2}$ and good cycling stability upon illumination by a white LED with a power of 70 $mW cm^{-2}$.

3.2.1.2 | Carbon Nanotubes. Carbon nanotubes (CNTs) are another huge class of porous carbon nanomaterials generally classified in single-walled (SWCNTs) or MWCNTs depending on the number of graphene layers. Their distinctive mechanical and thermal stability, unique porous structure, and high conductivity made them suitable high-power electrodes in SC [124].

More specifically, CNTs are characterized by networks of interconnected mesopores, which facilitate the diffusion of the electrolyte, hence resulting in lower equivalent series resistance (ESR) values than AC [125, 126]. Owing to the great conductivity and the accessible pores, CNTs can accumulate charges via non-Faradaic mechanism—making them EDLCs—but the lower specific surface area compared to AC ($<500 m^2 g^{-1}$) leads to lower E_d [2]. Typical PCs leverage the mechanical and electrical properties of CNTs by hybridizing them with other materials such as conductive polymers or metal oxides. Already in 2012, Peng and coworkers reported the use of polyaniline (PANI) to coat a MWCNTs film, thus obtaining a PANI-MWCNTs composite, that showed a boosted specific capacitance of 208 $F g^{-1}$ in comparison with the 48 $F g^{-1}$ of the sole MWCNTs electrode [40]. The overall photoelectric conversion and storage efficiency however dropped from 5.12% to 4.29% upon PANI incorporation, probably due to reactions of the polymer with the CNTs. A later work by Liu et al. reported a 2T SC made by self-supported graphene/CNT hollow fibers featuring a high PANI mass loading both on the inner and outer surface [41]. The material exhibited a specific capacitance of 472 $mF g^{-1}$ and was able to replace the Pt wire in fiber-shaped DSSC leading to a power conversion efficiency of 4.20% and an overall efficiency of 2.1% of the integrated PC. The light-assisted symmetric supercapacitor fabricated by Momeni et al. that featured hydrothermally synthesized WO_3 , already mentioned in Section 3.1, integrated this metal oxide with MWCNTs [27]. The initial MWCNTs- WO_3 supercapacitor was sandwiched between a graphite layer and an FTO glass showing specific capacitance of 47 $mF cm^{-2}$ and a 25% increase in capacity under illumination, surpassing the performances of the pure WO_3 electrode. In PBs, CNTs are incorporated into the photoelectrode materials since they are able to significantly improve the photovoltaic conversion efficiency by reducing the recombination of the excitons and accelerating the electron transport. CNTs have been successfully used as photocathodes in Li- CO_2 batteries in combination with carbon nitride [42] and in Zn-ion batteries as covalent-organic-framework/carbon nanotubes (COF/CNTs) hybrids [43].

3.2.1.3 | Graphene and Derivatives. Graphene and its derivatives, such as graphene oxide (GO) and rGO, are a paramount category of carbon nanomaterials for the development of PSCs. Graphene is one of the most common electrode materials for energy storage devices since it combines high specific surface areas and strong electrical conductivity with excellent mechanical stability and flexibility, necessary for wearable electronic devices. On the other hand, the oxygen-containing functional groups of GO make it a suitable semiconductor for light absorption in the visible range, and the partially restored sp^2 carbon system of rGO enhances the conductivity and lowers the energy barriers for photoelectron transfer from photosensitive materials (e.g., perovskites) [10]. Therefore, graphene is commonly used alone or in combination with conductive polymers or metal oxides in SCs, where it stores charges acting as an EDLC [44]. Instead, rGO can function both in the SC part as conductor [45] or in the PV component as supportive material or electron transporting layer [127]. The versatility of graphene and its derivatives made possible their integration into a wide range of different architectures and devices. Plenty of reviews have been published in the latest years summarizing the progress done with these materials and their composites in PCs and PSCs with

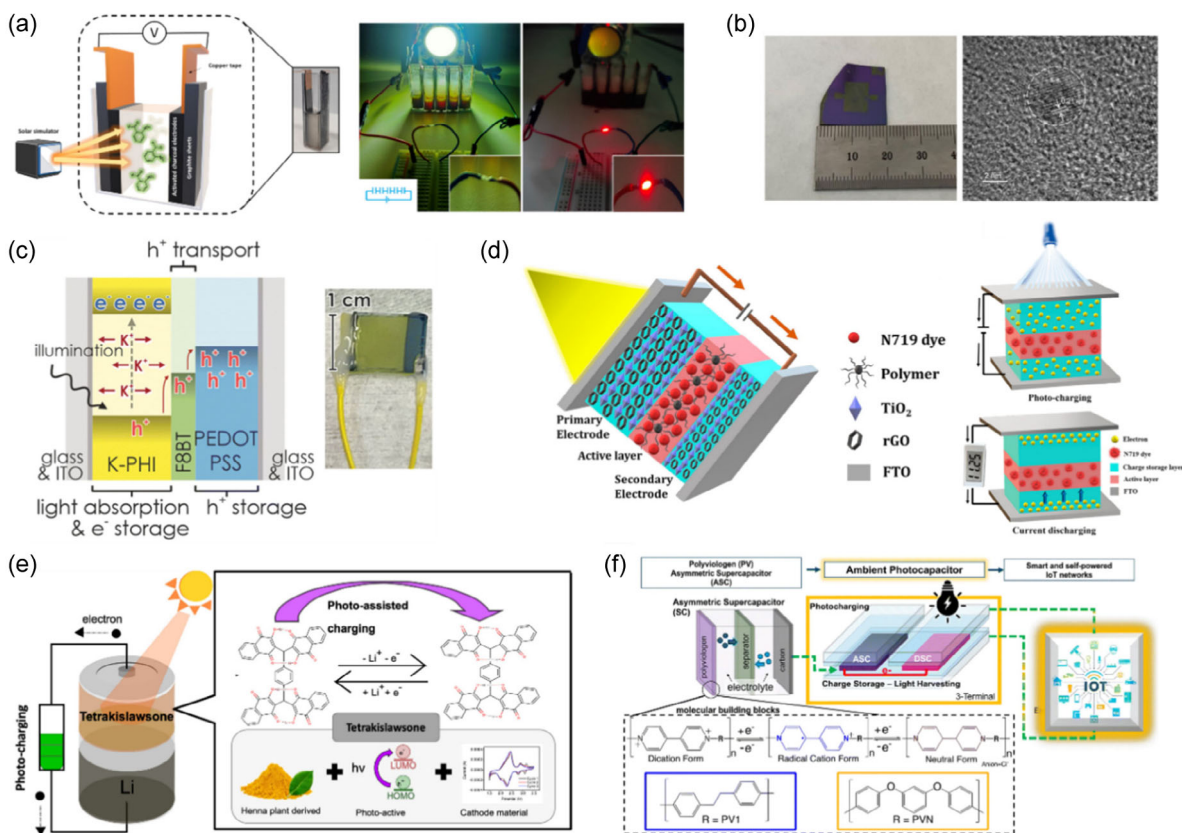


FIGURE 3 | Examples of organic materials use in PCs/PSCs and PBs. (a) Scheme of a 2T PC built in the cuvette, which was used to power a small red LED after photo-charging under white light. Reproduced under the terms of CC-BY 4.0 license [34], Copyright 2025, Wiley. (b) Digital photo of a planar micro-supercapacitor on a Si wafer (left) and high-resolution TEM image of graphene quantum dots (right). Reproduced with permission [35], Copyright 2025, American Chemical Society. (c) Schematic illustration (left) and digital photo (right) of a direct PB featuring K-PHI as electron storage material, F8BT as hole transport material and PEDOT:PSS as hole storage material. Reproduced under the terms of CC-BY 4.0 license [36], Copyright 2023, Royal Society of Chemistry. (d) A compact PSC configuration exploiting rGO and a dye in the active layer and of the charging-discharging processes. Reproduced with permission [37], Copyright 2025, American Chemical Society. (e) Schematics of a PB with lithiated TKL as photocathode and detail of the light-assisted reactions that take place during charge-discharge cycles. Reproduced with permission [38], Copyright 2021, American Chemical Society. (f) An ambient PC with the detail of the reversible redox reactions and the chemical structures of the polyviologen polymers used in the asymmetric device. Reproduced under the terms of CC-BY 3.0 license [39], Copyright 2024, Royal Society of Chemistry.

various architectures [5, 7, 128–131]. Concerning the PBs, graphene demonstrated to be useful in the PV unit for suppressing the back-transport reaction, leading to higher energy conversion efficiencies [132]. rGO, instead, was used in combination with V_2O_5 by Boruah et al. in 2-electrode solar-driven Zn-ion batteries, leading to an enhancement in the transport of the photogenerated electrons [133]. A recent research field under exploration is related to microsupercapacitors (micro-SC), which basically represent traditional SC at the microscale, investigated as miniaturized energy storage devices for flexible microelectronics [134]. Suitable candidates materials in such context are graphene quantum dots (GQDs), nanoscale fragments of graphene with improved electrical conductivity and high specific surface area. They have lately been applied by Zhang and coworkers in combination with graphene to build a planar micro-SC (Figure 3b) with a 2T architecture via photolithography, reaching a characteristic frequency of 51,379 Hz and a noteworthy output P_d of 14.76 W cm^{-2} [35]. GQDs also demonstrate tunable photoluminescence properties due to the quantum confinement effect and show light adsorption over a broad range of wavelengths in the visible spectrum. That is why they have been used as sensitizers in DSSCs [135] and as the active layer in organic PV devices [136].

Differently from the carbon nanomaterials previously introduced, which found most of the applications in PCs and PSCs, graphitic carbon nitride ($g\text{-C}_3\text{N}_4$, or simply CN) has been investigated mainly for PBs. For instance, in 2015, Liu et al. reported for the first time the use of this material in a LiO_2 battery, where it acted as photocatalyst to reduce the charging voltage [137]. More recently, the group of Lotsch showed that potassium poly(heptazine imide) (KPHI), an ionic derivative of CN, could be used as bifunctional solar battery photoanode combined with organic hole transfer and storage materials (Figure 3c) [138]. They found that simultaneous energy conversion and storage could be achieved in a single device with a round-trip efficiency of 94%.

3.2.2 | Dyes and Photosensitive Organic Molecules

The core aspect of PCs and PBs that differentiate them from standard and well-known SCs and batteries is the capability of storing energy from the photons. Therefore, efficient solar harvesting and light absorption over a broad spectral window is a pivotal requirement for the development of these devices. Key technology in the field are DSSCs, which rely on the use of dyes and photosensitive organic molecules. These organic compounds

are usually adsorbed on the surface of a wide band semiconductor (usually TiO_2) acting as sensitizers. In a typical DSSC-based PC, dye molecules are photoexcited by absorbing the incoming photons and inject the excited electrons into the conduction band of the TiO_2 photoanode. The photogenerated electrons are transported through an external circuit to the counter electrode and finally stored in the charge storage unit, while the oxidized dye is reduced back to its neutral state thanks to electron transfer for the redox couple (typically I_3^-/I^-) present in the electrolyte [139]. Since this process is critical for continuous charge generation, an ideal photosensitizer must meet important criteria such as broad spectral coverage, suitable energy level alignment, and good stability and adherence to the TiO_2 [140]. Thanks to their facile and cheap fabrication, transparency, and excellent efficiency even under indoor light conditions, DSSCs have been a pivotal component of PCs for years. In 2004, Miyasaka et al. exploited a DSSC based on the Ru complex dye *cis*-bis(isothiocyanato)bis(bipyridyl)-dicarboxylato-ruthenium(II)bis-tertabutylammonium to build the first documented solar-charged SC system [1]. Since then, the research on PCs and PSCs leveraged a huge variety of dyes and photosensitive organic molecules as sensitizers, which have also been applied as photocathodes in PBs. They can be categorized mainly into metal-based complexes, metal-free organic dyes, and natural dyes [130]. For the broadness of the topic, the discussion herein is limited to selected PCs and PBs devices with a 2-electrode setup of recent works. The readers interested in a wider report on dyes and PCs with other architectures are addressed to the review of Freitag et al. [79] as well as on the newly released one by Li et al. [18]. Among the metal-based dyes, Ru complexes are the most effective sensitizers. In particular, the Ru-polypyridyl complexes were able to achieve excellent photoconversion efficiencies thanks to the geometrical structure of the ligand, tunable photo(electro)chemical properties, chemical stability, and solubility [1, 141]. A recent review was written by Colombo et al. exploring the latest advances on Ru-complexes in DSSCs [142]. In PC devices, two of the most used Ru-based dyes are N3 and N719. The latter was chosen as photoactive material by Surana and coworkers to fabricate a new 2-electrode PC (Figure 3d) where both electrodes have a layered architecture of rGO and TiO_2 [37]. They reported a specific capacitance of 20.3 F g^{-1} , which was more than doubled when the back electrode was substituted with simple conductive carbon (43.5 F g^{-1}). Metal-free dyes and natural dyes are often preferred to metal complexes as more eco-friendly and low-cost alternatives. The former are synthesized with an electron donor moiety (D) bridged to an electron acceptor one (A) by a π system creating a D- π -A structure. The researchers, however, focused on application in solar cells rather than compact PCs and PSCs, hence leaving this field open for future integration of the already studied DSSCs into photo(super)capacitors [130, 143, 144]. The latter have also been rarely explored for the production of PCs, with only one noteworthy work from Das et al., where hibiscus dye served as co-sensitizer for TiO_2 together with CdS quantum dots [145]. However, natural dyes found a more successful field of application in PBs. For instance, tetrakislawsonone (TKL)—a naturally occurring quinone-based compound—was employed by Kato and coworkers in a Li-ion PB (Figure 3e) as material with dual functionality: charge storage and light harvesting [38]. Upon light absorption, lithiated TKL generated electron-hole pairs: the holes oxidized the lithiated TKL to TKL, while the electrons flowed to the Li anode. The authors observed a rise in charging

current, specific capacity, and Coulombic efficiency under irradiation, thus assessing the dual function of TKL.

3.2.3 | Conductive Polymers

Conductive polymers are highly conjugated molecules that can give a fast delocalization of electrons along their backbone, thus possessing intrinsic conductivity that facilitates electron transport [2]. These properties make them important pseudo-capacitive materials, which store charges via fast and reversible Faradaic redox reactions both in the surface and in the bulk of the electrode. Hence, conductive polymers can dramatically increase the specific capacitance of SCs reaching higher capacitance values than EDLCs, which store charges via non-Faradaic processes [146, 147]. These characteristics, along with their intrinsic flexibility and facile hybridization with carbon nanomaterials or metal oxides, are crucial in the development of high-performance and wearable PSCs. Conductive polymers have been used across several PSCs devices, acting as counter electrode in the PV unit or, more often, as charge storage electrode in for the PSC unit in integrated 2T architecture [15]. They have also been leveraged in PBs principally as hole-transporting layers or pseudocapacitive cathodes thanks to their ability to coordinate energy harvesting, charge transport, and charge storage [148]. The most commonly employed polymers in PSCs include polyaniline (PANI), polypyrrole (PPy), (3,4-ethylenedioxythiophene) (PEDOT), and their composites. Yet, the field is rapidly expanding toward other molecules and hybrids that will be shortly discussed. PANI is obtained by the polymerization of aniline monomers, and it is frequently chosen for its pseudocapacitive properties and ease combination with carbon materials. Back in 2015, polyaniline was used by Yin et al. to build one of the first noteworthy examples of all-in-one 2-electrodes PSC [149]. The authors fabricated a dual-acting electrode using PANI/CNTs film, which was able to simultaneously convert and store solar energy without the need for a PV integration, thus achieving specific capacitance of 140 F g^{-1} . The use of PANI as a coating for nanocarbon or stainless-steel wires in was reported in several other works on 2T PSCs, always resulting in improved capacitive behavior [41, 40, 150, 151]. In the field of PBs, a recent work by Chen et al. reported a novel photorechargeable Al battery with PANI photoelectrodes and safe ionic liquid electrolyte [152]. The device presented enhanced reversible specific capacity of $\approx 191\%$ over 500 cycles under illumination in the range of wavelength 320 nm to 780 nm. PPy is synthesized by oxidative polymerization of pyrrole, and it is characterized by high conductivity, stability, and flexibility. For these reasons, it has been extensively used as charge storage electrode in DSSCs-based [153] or perovskite-based [12] 2T systems that leveraged its pseudocapacitive behavior. A new work by Momeni et al. reported the fabrication of a flexible and lightweight symmetric 2T PSC with a dual photoelectrode, which was produced by photoelectrochemical deposition of Te on a PPy- V_2O_5 film [154]. The final device used PVA-LiCl electrolyte and reached specific capacitance values of 131 mF cm^{-2} and 45 mF cm^{-2} at 1.0 and 3.0 mA cm^{-2} respectively, with an excellent retention of 93% of capacitance after over 12 000 cycles. PEDOT is the polymer of 3,4-ethylenedioxythiophene, and it is often coupled with polystyrene sulfonate (PSS) to form a PEDOT:PSS composite where PEDOT provides electrical conductivity and PSS enhances stability and processability. PEDOT alone has been used in PBs [153] and

2T PCs [154] as charge storage electrode. The composite PEDOT:PSS, thanks to its flexibility and facile manufacturing, was frequently adopted for flexible 2T PC devices [155, 156]. Lately, Gouder et al. adopted PEDOT:PSS as the hole-storage material cathode layer in a K-PHI-based solid-state solar battery [36]. The polymer composite operated by reductively quenching the holes photogenerated by the *n*-type K-PHI. Thus, the final device showed an increase in the energy and charge output by 60% and 63% respectively under 1 sun illumination. The versatility of this material is also fostering research in other fields, such as organic photovoltaics [157], bioelectronics [158], and thermoelectric applications [159]. In addition to these traditional conductive polymers, researchers have investigated other materials that can be suitable for the next-generation PCs and PSCs. Lately, Florez-Diaz et al. have employed for the first time polyviologens (PVNs) to build a new asymmetric SC and integrated it with a DSSC in a 3T PC [39]. Although lying outside of the purpose of this review, the three-electrode device worth mentioning for its innovative choice of the materials, performances, and real-life application. Indeed, the so called “ambient photocapacitor” (Figure 3f) achieved formidable power conversion and photo-charging efficiencies of more than 30% and 18%, respectively, and proved to reliably power a multilayer IoT network at 500 Lx for 72 h. All these findings show how the field of polymer-based photo(super)capacitors is in rapid and incremental expansion, paving the way for new, adaptable, and more sustainable power-sources for the technology of tomorrow.

4 | Electrolytes

The electrolyte is a key component in energy conversion and storage devices, as it enables charge transfer and the movement of electrons and holes. While many studies have focused on electrolytes in PBs and PSCs [48, 49], a detailed discussion of this topic is outside the scope of this review. However, it is still relevant to outline the main types of electrolytes used in PBs and PSCs. These can generally be divided into three categories based on their physical state: solid, gel, and liquid electrolytes, each with its own benefits and drawbacks. In the study by Chauhan et al., a significantly enhanced electrochemical capacitance was reported when using a liquid electrolyte compared to a solid-state one in a ZnO nanowire-based PSC [50]. As previously mentioned in the Section 4, an innovative contribution by Morag and coworkers demonstrated a self-chargeable PSC employing a photosensitive organic electrolyte—specifically, 2-nitrobenzaldehyde dissolved in 0.5 M H₂SO₄, to improve ionic conductivity. This electrolyte enabled a high C_s and excellent cycling stability in a simple device based on activated carbon electrodes [34]. Sulfuric acid is frequently used in aqueous-based electrolytes, as in the previously mentioned WO₃/MWCNTs asymmetric PC, where a PVA/H₂SO₄ gel electrolyte was adopted [27]. Remaining within the framework of WO₃ as a photoactive material, a mixture of ethylene carbonate and diethyl carbonate was employed as the electrolyte in a Li-ion PB, leading to the formation of a solid–electrolyte interface upon charge separation [23]. The same electrolyte was also applied in the Cs₃Bi₂I₉ PIM-based PB in the work of Tewari et al. [53]. Overall, aqueous electrolytes are commonly employed in PCs and PSCs based on TMOs or MSs, particularly when these materials are not integrated with carbon-based structures. The relevance of such electrolytes lies

in their environmentally friendly nature, which enables the development of sustainable systems suitable for wearable devices or indoor light-harvesting applications. The main limitation of employing aqueous electrolytes, especially in PCs and PSCs, is represented by the operating voltage, theoretically restricted to 1.2 V owing to the occurrence of water splitting. Nonetheless, several strategies can be adopted to overcome this limit [160]. This represents a promising direction for future research, opening new opportunities for practical implementation. Nevertheless, it should be noted that in many cases, charge-transfer properties are significantly enhanced when using organic electrolytes. This improvement is often associated with the frequent use of carbon-based materials in energy storage devices, which typically require organic-type electrolytes to achieve satisfactory performances. Although certain organic electrolytes may raise toxicity concerns, these can be mitigated by adopting polymer-based gel electrolytes, even if their implementation may demand additional engineering in device fabrication. In ion-based PBs, the electrolyte typically contains metal ions, as summarized in Table 1 (*vide infra*). Since the electrolyte composition is strongly interconnected with the overall device architecture and performance, it deserves a critical investigation alongside the study of the photoactive materials. A concise overview of the most employed electrolytes is provided in Tables 1 and 2 (*vide infra*) [161, 162].

5 | CEs

Another critical aspect to be considered for assembled devices is the influence of the counter electrode (CE) on the overall performance. The intrinsically different operating mechanisms of PBs and PCs/PSCs require treating such component separately, for the two photo-charging systems. As summarized in Table 1, the most common configuration relies on metal-ion battery-type CEs, where the CE consists of a suitable metal and its corresponding ion. Among these, lithium-based systems remain the most widely studied, making Li/Li⁺ CEs a natural choice for integration with emerging photoactive electrodes and often resulting in high specific capacitances, as reported in Table 1 [21–23, 38, 41, 105, 110, 113]. Examples employing zinc/zinc-ion CEs are also reported, representing a viable alternative within the broader family of metal-ion configurations and offering performances comparable to those achieved with Li/Li⁺ systems [33, 43, 133]. Conversely, only a limited number of reports explore organic CEs; these studies nevertheless illustrate that highly variable outcomes can be obtained depending on the nature and compatibility of the materials constituting the full device [36, 138].

In the context of PCs/PSCs, the role of the CE must also be considered in relation to the device architecture. As illustrated in Figure 1d, e, two main configurations are possible, depending on the composition of the CE. In asymmetric PCs [27, 31, 46, 47, 54, 96] (Figure 1d), the CE material differs from that of the photoactive electrode, whereas in symmetric PCs [154] (Figure 1e), both electrodes are constructed from the same material, allowing illumination from either side of the device. Although this bidirectional illumination can be considered an added advantage, its practical impact is often limited by the use of transparent conductive substrates (e.g., fluorine-doped tin oxide) as current collectors, which generally exhibit lower

TABLE 1 | Performances comparison between different 2T PBs based on photoactive materials described in the review.

PE	CE	Electrolyte	PCE, % ^a	C _s ^b	J	C _R , % ^b	Cycles	E _d ^b	P _d ^b	References
Cu ₂ O/TiO ₂	Li/Li ⁺	LiPF ₆ 1M in EC:DEC (1:1)	n.a. ^c	146 mAh g ⁻¹	0.1 C	n.a.	n.a.	n.a.	n.a.	[22]
V ₂ O ₅ /P3HT/rGO	Li/Li ⁺	LiTFSI 1M	0.22 2.6 (455 nm)	127 mAh g ⁻¹	300 mA g ⁻¹	n.a.	n.a.	n.a.	n.a.	[21]
WO ₃ /Graphite	Li/Li ⁺	LiPF ₆ 1M in EC:DEC (1:1)	5.96	1150 mAh g ⁻¹	0.1 C	n.a.	n.a.	n.a.	n.a.	[23]
TiS ₂ /TiO ₂	Li/ILi ⁺	20% LiClO ₄ in Polyethylene oxide	0.229 (white LE, 70 mW)	586 mAh g ⁻¹	n.a.	n.a.	n.a.	n.a.	n.a.	[105]
Ag _{0.5} Cs _{0.5} Bi ₃ I ₁₀	Zn/Zn ²⁺	ZnSO ₄ 2 M in H ₂ O	2.1	321 mAh g ⁻¹	0.5 Ag ⁻¹	76	1000	n.a.	n.a.	[33]
Cs ₃ Bi ₂ I ₉	Li/Li ⁺	LiPF ₆ 1 M in EC:DEC (1:1)	0.43	975 mAh g ⁻¹	100 A g ⁻¹	n.a.	n.a.	0.075 mWh cm ⁻²	100 mW cm ⁻²	[53]
Cs ₃ Bi ₂ Br ₉ /TiO ₂	Pt	All solid-state	0.03	n.a.	n.a.	n.a.	n.a.	n.a.	n.a.	[55]
LiFePO ₄ /TiO ₂	Li/Li ⁺	LiPF ₆ 1 M in EC:DEC (1:1)	n.a.	ca 220 mAh g ⁻¹	0.5 C	n.a.	n.a.	n.a.	n.a.	[113]
CNT/C ₃ N ₄	Li/Li ⁺	Ionic gel	n.a.	15.77 mAh cm ⁻²	0.10 mA cm ⁻²	n.a.	n.a.	n.a.	n.a.	[41]
TN-COF/CNT	Zn/Zn ²⁺	Zn(CF ₃ SO ₃) ₂	n.a.	n.a.	50 mA g ⁻¹	n.a.	n.a.	n.a.	3.16 mW cm ⁻²	[43]
V ₂ O ₅ /P3HT/rGO	Zn/Zn ²⁺	Zn(CF ₃ SO ₃) ₂ 3 M in H ₂ O	1.2 (455 nm)	370 mAh g ⁻¹	50 mA g ⁻¹	n.a.	n.a.	n.a.	n.a.	[133]
K-PHI/PVK	PEDOT/PSS	KCl 0.1 M in H ₂ O	n.a.	3.1 Ah kg ⁻¹	5.01 A kg ⁻¹	n.a.	n.a.	2.4 Wh kg ⁻¹	n.a.	[138]
K-PHI/F8BT	PEDOT/PSS	KCl 0.1 M in H ₂ O	0.002	2.3 mAh g ⁻¹	10.5 mA g ⁻¹	98	50	n.a.	n.a.	[36]
Tetrakislawsonone (TKL)	Li/Li ⁺	LiTFSI 1 M in PP 13TFSI	n.a.	332 mAh g ⁻¹	50 mA g ⁻¹	n.a.	n.a.	n.a.	n.a.	[38]
PANI	Al	Ionic liquid of AlCl ₃ :[EMIm]Cl (1:3)	n.a.	133.3 mAh g ⁻¹	100 mA g ⁻¹	n.a.	n.a.	n.a.	n.a.	[152]

^aIf not differently reported PCE, C_s, E_d, and P_d are evaluated under 1 sun illumination.
^bIf not differently reported C_s, C_R, E_d, and P_d are evaluated under 1 sun illumination, with current charging.
^cNot available data.

TABLE 2 | Performances comparison between different 2T PCs based on photoactive materials described in the review.

PE	CE	Electrolyte	C_s^a	J	C_R^b % ^a	Cycles	E_d^a	P_d^a	References
$Fe_{1.84}V_{0.16}O_3$ NPs	Fe/PVDF	KOH 6 M in H ₂ O	172.8 mAh g ⁻¹ ^b 23.8 mAh/g	5 Ag ⁻¹	63.5	50	22.9 Wh/kg	4852.6 W kg ⁻¹	[96]
$Fe_{1.84}V_{0.16}O_3$ NPs	Stainless steel	Fe ²⁺ /TEGDME	496.6 mAh/g	500 mAh g ⁻¹	80.3	100	13.26 Wh kg ⁻¹	95 W kg ⁻¹	[96]
WO_3 /MWCNTs (FTO)	WO_3 /MWCNTs (Graphite)	PVA/H ₂ SO ₄ gel	92.72 mF cm ⁻² 231.8 F g ⁻¹	1 mA cm ⁻²	n.a. ^d	n.a.	n.a.	n.a.	[27]
ZnO NWs	ZnO NWs	PVA/LiCl	39.1 mF g ⁻¹	1.1 mA g ⁻¹	98.9	3000	78.1 mWh kg ⁻¹	n.a.	[102]
ZnO/16% rGO	Carbon paper	PVA/LiCl	40 mF cm ⁻²	0.4 mA cm ⁻²	98.9	3000	22 μWh cm ⁻²	0.36 mW cm ⁻²	[103]
ZnO/MWCNTs	Ag	KOH	2260 mF g ⁻¹ ^b ca 2000 mF g ⁻¹	at 12 mA g ⁻¹	88	1500	313 mWh kg ⁻¹ ^b	ca 8 W kg ⁻¹ ^b	[54]
MnNiCoS	MnNiCoS/TiO ₂	Ethylene glycol	789 mF cm ⁻²	at 1 mA cm ⁻²	84.7	10 000	4551 mWh cm ⁻²	n.a.	[31]
CdS/NiCo ₂ S ₅	Activated carbon	KOH hydrogel	400.8 F g ⁻¹	3 Ag ⁻¹	75	3000	95.6 Wh kg ⁻¹	2869 W kg ⁻¹	[25]
$FeCo_2O_4$ /Bi ₂ S ₃	Zn/Zn ²⁺	ZnSO ₄	744 mF cm ⁻²	0.3 mA cm ⁻²	97.59	10 000	413.33 mWh cm ⁻²	882.67 mW cm ⁻²	[46]
MoS_2 /NaTaO ₃	Zn/Zn ²⁺	Zn (CF ₃ SO ₃) ₂ 3M	93.94 mF cm ⁻² ^c	—	96	4000	n.a.	n.a.	[47]
CdS/ZnO	Ag	Zn(CF ₃ SO ₃) ₂ 3M in H ₂ O	ca 50 mAh g ⁻¹	500 mA g ⁻¹	99%	1000	ca 30 Wh kg ⁻¹	ca 100 W kg ⁻¹	[29]
MnS/V_2O_5 /BiVO ₄	MnS/V_2O_5 /BiVO ₄	PVA/KCl polymer gel	ca 38 F g ⁻¹	0.07 mA cm ⁻²	ca 100	3000	7 Wh kg ⁻¹	250 W kg ⁻¹	[28]
MoCo/BiVO ₄	Graphite	PVA/KCl polymer gel	240 mF cm ⁻²	0.15 mA cm ⁻²	ca 100	3000	270 mWh cm ⁻²	0.15 mW cm ⁻²	[26]
rGO/TiO ₂ (3 layer each)	Carbon	N719/Pluronic F127/ACN	43.5 F g ⁻¹ (0.3 sun)	4 mA g ⁻¹	93	50	n.a.	n.a.	[37]
Te/PPy/V ₂ O ₅	Te/PPy/V ₂ O ₅	PVA/LiCl polymer gel	131 mF cm ⁻²	1 mA cm ⁻¹	93	12 000	n.a.	n.a.	[154]

^aIf not differently C_s , C_R , E_d , and P_d are evaluated under 1 sun illumination, with current charging.

^bEvaluated from CV, at 5 mV/s.

^cEvaluated from CV, at 10 mV/s.

^dNot available data.

conductivity and electrochemical performance compared with metal-based collectors such as titanium or copper foils. Table 2 compiles the range of CE materials employed in PCs/PSCs alongside their corresponding device performances, showing that both the intrinsic properties of the CE and its interaction with the full device architecture critically affect the electrochemical behavior.

6 | Device Performance

When analyzing 2T devices, it immediately becomes evident that comparing their performances and identifying the key strengths of the selected materials is a challenging task. This difficulty primarily arises from the absence of standardized protocols that would allow a rapid and transparent evaluation of the complete device characteristics. This issue stems from the fact that each device represents a combination of multiple components, such as the photoactive material, conductive substrate, electrolyte, separator, and counter electrode, all of which collectively influence the overall working mechanism and performance. Therefore, it is essential to consider all relevant variables and parameters used in each study and to clearly recognize the limitations of the compared examples. In the Figure 4a, it is summarized a schematic representation of a 2T photo-rechargeable device, presenting the important

parameters (on the left) related to the photoactive electrode, with its energy conversion functionality, and the characteristic performances of the counter electrode, which together with the charge transport material, and the other components, is responsible of the energy storage functionality. The highlighted PCE and C_s of some devices explored in this review are reported in Figure 4b–d. To facilitate comparison and provide a clearer overview, two summary tables are presented at the end of this section, highlighting the main features and performance trends of the devices discussed in this review (Table 1 for PBs and Table 2 for PCs).

6.1 | Photo Conversion Efficiency (PCE)

This parameter is a key metric in photo-rechargeable devices, as it indicates how efficiently a material can convert incident sunlight into electrical energy under operating conditions. Sunlight contains photons spanning a broad range of energies, yet only photons with energies above the material's bandgap can be absorbed and contribute to current generation [164]. Consequently, PCE is almost always reported in studies focusing on energy conversion systems, including solar and photovoltaic cells, since it is one of the most important performance indicators. The upper efficiency limit is fundamentally constrained by the Shockley–Queisser limit for the specific bandgap. Light-to-energy conversion efficiency

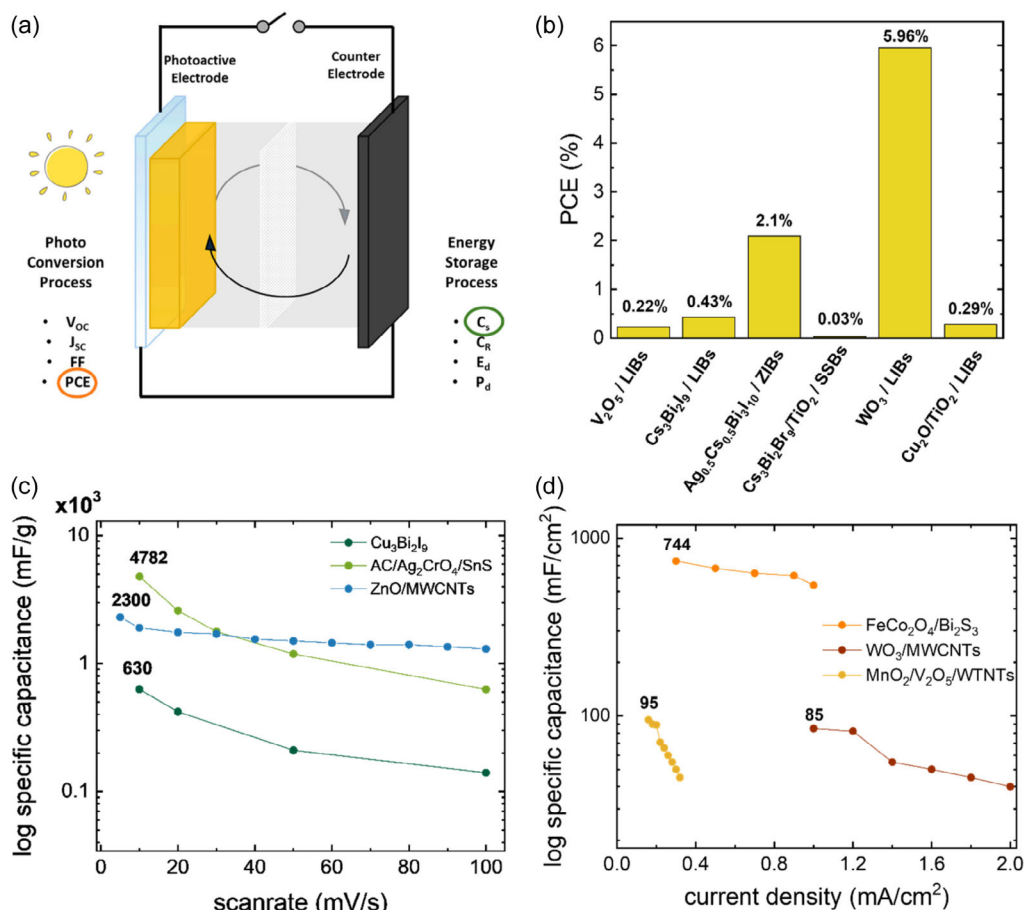


FIGURE 4 | (a) Schematic representation of a 2T photo-rechargeable device, with important parameters used to evaluate the light harvesting unit and the energy storage unit; (b) PCE comparison between different photoactive materials-based PBs under 1 sun illumination [21–23, 33, 53, 55]; (c) C_s trend against scanrate between different photoactive materials-based PCs, performed under 1-sun illumination [24, 54, 112]; and (d) C_s trend against current density between different photoactive materials-based PCs, performed under 1-sun illumination [27, 46, 163].

depends strongly on both the material properties and the device configuration, mainly due to different loss mechanisms [165, 166]. PCE represents the fraction of incident light converted into electrical energy, making it essential to clearly specify the illumination conditions used during testing. While solar simulators are most employed, LED-based illumination is also used in some studies. However, the PCE measured under 1-sun illumination can differ significantly from that obtained under LED light, depending on the spectral range that the material can effectively absorb. The duration of continuous illumination is another key factor influencing device performance. Prolonged light exposure can lead to increased temperature, which may cause a decline in PCE and induce structural or compositional changes in the active material. Therefore, both the illumination type and duration must be carefully controlled and reported to ensure reliable evaluation and comparison of device performance. Examining a fully integrated device capable of both converting sunlight into electrical energy and storing it, the energy storage subsystem becomes a critical component to assess. Consequently, several studies place increased emphasis on the storage performance and intrinsic properties of the selected materials, neglecting the harvesting aspect. PCE is, when reported, evaluated as in a photoconversion system, considering only the harvesting unit performance and it is deeply different from the photocharge efficiency (or overall energy conversion efficiency, OECE), which considers both the conversion and storage process, and which is of course derived from different parameters according to the electrostatic charge system of a PC and a chemical charge system of a PB. The development of a clear protocol for the evaluation of PCE and OECE for 2T devices is necessary to provide a reliable insight on their performances. PCE is in some cases evaluated in PB-type devices: Accordingly, we present, in Figure 4b, a comparative plot of the PCE values obtained under one-sun illumination for different photoactive materials of interest. It is evident the promising PCE of the WO_3 based electrode in Li-ion batteries obtained from Sajjad and coworkers, reaching a value of almost 6% [23].

6.2 | Specific Capacitance (C_s)

The primary parameter used to assess the performance of an energy storage device is the C_s , which represents the amount of charge that can be stored relative to the amount of active material, in terms of mass or area. A higher C_s indicates superior capacitive behavior of the electrode material and, consequently, improved overall device performance. Accordingly, a major focus of current research in the energy storage field is the identification of suitable materials and the optimization of device architectures to enhance C_s emphasizing the central importance of this parameter in determining system efficiency [56, 119]. Moreover, C_s is typically enhanced under illumination, owing to storage of photogenerated charges, resulting, in 2T devices, in a deep interconnection of this parameter with the light harvesting ability of the active material. For this reason, the comparison of C_s values retrieved via tests performed in dark and under illumination can provide an initial evaluation of the device photo storage performance. Energy storage devices are frequently based on 2D materials, as it is well established that a larger surface area enables the accumulation and storage of a higher amount of charge. For this reason, C_s is often reported with respect to the surface area of the functional electrodes. While this approach is

informative, it is not directly comparable to C_s values calculated on the basis of the active material mass loaded onto the conductive substrate, which is also a common practice in some studies. The gravimetric capacitance, as well as parameters as E_d and P_d (Section 6.3), are often reported for systems presenting very small mass of active material, leading to exceptionally high, but misleading, performances [167]. The evaluation of $C_s/E_d/P_d$ variation with different mass loading could offer an insight on how the active mass influences the computation of these parameters. The charge storage capacity of a material can be improved by adjusting various parameters related to device engineering. Therefore, it is important to consider factors such as the counter electrode configuration (and, in PCs/PSCs, whether the device is symmetric or asymmetric), the electrolyte, the separator, and the charge storage mechanism, which, as discussed in Section 1, differs depending on whether the device behaves as a (super)capacitor or as a battery. Each material may respond differently to these parameters, requiring careful optimization of the device architecture to achieve the best performance. Reporting C_s , it is important to consider the influence of the experimental parameters used, as they have a significant impact on the resulting values. C_s is often expressed as a function of the scan rate in CV measurements or as a function of current density in galvanostatic charge–discharge (GCD) experiments. These two methods provide different approaches to determine this data, often yielding slightly different values. Consequently, direct comparisons between capacitances obtained from CV and GCD are not straightforward, representing an additional challenge in evaluating different devices. Given these discrepancies, it is crucial to identify the most accurate procedure to extract realistic capacitance values. Studies have been dedicated to this topic, aiming to establish a reliable protocol for performance evaluation in the future [57]. In this review, we present the C_s trends of selected materials measured under comparable conditions, allowing for partial comparison. These results are summarized in Figure 4c,d, noting that all data refer to PC-type devices. From these graphs the Ag_2CrO_4 coupled with SnS [112] presents an incredibly high C_s compared to the other evaluated from the CV, highlighting the already discussed importance of TMOs coupled with MSs. Based on GCD measurements, the device presenting the $\text{FeCo}_2\text{O}_4/\text{Bi}_2\text{S}_3$ heterojunction [46] reach a C_s of 744 mF cm^{-2} , quite high value than the others presented, confirming as written above. The impossibility of comparison between the two graphs suggests the necessity of standard operating condition, and the C_s obtained from a CV measure could be a good compromise, since different material can hold up different current density values.

6.3 | Energy and Power Densities

E_d and P_d represent critical metrics for energy storage devices, as they define the operational differences between supercapacitors and batteries, and thus between PCs/PSCs and PBs. Batteries typically exhibit higher E_d , enabling the storage of large amounts of energy, albeit with slower charging rates, while supercapacitors offer higher P_d , supporting rapid charge and discharge. This trade-off leads to distinct performance profiles, guiding the selection of device type based on the application requirements. The ongoing challenge in the field is to enhance the parameter in which a device is intrinsically limited, E_d in supercapacitors or P_d in batteries [58]. In photo-rechargeable systems, the large

amount of parameters that could be considered can sometimes overshadow the evaluation of energy and P_d , although their understanding may suggest whether supercapacitors or electrical double-layer capacitors could ever match the performance of batteries, a goal not yet achieved [59]. As reported in Table 1, in the context of PBs these parameters are not commonly evaluated, but it could be seen that the P_d are in the order of 1–100 mW cm⁻², while E_d vary from 0.075 mWh kg⁻¹ [53] to 2.4 Wh kg⁻¹ [138]. On the other hand, PCs/PSCs studies often present these quantities, as reported in Table 2: There are wide ranges of values, going from 0.15 mW cm⁻² [26] to 4852.6 W kg⁻¹ [96] for P_d , and from 22 μWh cm⁻² [103] to 95.6 Wh kg⁻¹ [25] for E_d . In Table 1 and 2 are reported the specific current condition in which these parameters are measured because it strongly influences the results.

6.4 | Cycle Stability

Device lifetime is another critical aspect to consider when evaluating energy storage systems. Supercapacitors generally exhibit remarkable cycle stability, often retaining their performance over hundreds of thousands of charge–discharge cycles, while batteries typically last only thousands of cycles. As a result, direct comparisons between PCs/PSCs and PBs are not straightforward; nevertheless, lifetime provides important insight into the reliability of the storage system and enables meaningful comparisons among different material-based devices. Long-term performance is typically assessed by monitoring C_s retention over cycling, usually derived from GCD experiments. There is no universally defined number of cycles; researchers generally select a cycle count sufficient to demonstrate the material's ability to maintain acceptable capacitance over extended operation.

In PBs, the C_R remains acceptable usually after some thousands of cycles of charge and discharge, even if not very high, as in the Ag_{0.5}Cs_{0.5}Bi₃I₁₀-based PB, presenting 76% of C_R after 1000 cycles [33]. In contrast, in PCs/PSCs the stability with cycles is almost always evaluated (as reported in Table 2) even in ten thousands of cycles, presenting for example values as 97.59% of C_R after 10 000 cycles [46], 99% after 10 000 cycles [29], and 93% after 12 000 cycles [154].

7 | Conclusions and Future Perspectives

In conclusion, based on our comprehensive survey of the literature and comparative analysis of state-of-the-art devices, we consider 2T geometry as the configuration with the highest potential for real technological deployment. In particular, the 2T design appears especially promising in applications where device compactness, mechanical flexibility and autonomous operation are essential, such as wearable electronics, soft robotic systems, implantable or skin-conformal biomedical patches, and self-powered IoT nodes for distributed sensing. The elimination of intermediate interconnections and functional separation maximizes photon-to-charge utilization and enables direct charge storage at the photoelectrode–electrolyte interface, a feature that is particularly advantageous in low-irradiance or intermittent illumination scenarios typically encountered in indoor IoT environments and on-body platforms. From our perspective, the 2T architecture also offers several intrinsic advantages over 3T and 4T configurations, particularly in terms of

integration and overall device compactness. In contrast, systems relying on multiple terminals or external wiring often experience increased resistive losses and greater structural complexity, which may hinder their implementation in scenarios that demand flexibility, miniaturization, and seamless integration. Furthermore, the reduced mechanical adaptability of 3T and 4T layouts limits their suitability for wearable or biomedical technologies, where conformability, tolerance to deformation, and intimate skin contact are critical to ensure consistent light harvesting and stable electrochemical performance. In these contexts, such architectures may face challenges in maintaining operational stability under continuous movement, bending, or variable illumination.

While acknowledging that each architecture offers specific advantages depending on the target application, current material innovations, for example hybrid photoactive systems, solid or quasi-solid electrolytes, and multifunctional nanostructured electrodes, strengthen our view that the 2T configuration represents a particularly promising route for next-generation integrated photo-rechargeable systems, especially where high integration density and functional synergy are key considerations.

Two-terminal PBs and PSCs embody an emerging frontier in solar energy research, where light absorption, charge separation, and electrochemical energy storage are seamlessly integrated within a single device. From a materials chemistry perspective, the rational design of photoactive electrodes should consider a synergistic balance between optical absorption, electronic conductivity, and electrochemical stability. The ideal materials must combine strong light-harvesting ability with efficient charge transport and long-term structural robustness under continuous illumination. This can be achieved through bandgap engineering, heterostructure formation, and nanoscale interface optimization, ensuring both high photoconversion efficiency and reliable energy retention.

On the engineering side, the two-terminal configuration offers structural simplicity and enhanced compactness compared to multiterminal or externally coupled systems, positioning it as a scalable platform for next-generation self-charging devices. However, critical challenges still need to be addressed, including mitigating charge recombination, reducing internal resistance, ensuring interfacial compatibility among dissimilar materials, and improving electrolyte stability under prolonged illumination. Furthermore, environmental and mechanical durability, including flexibility, moisture resistance, and operational stability under fluctuating light conditions, remain key bottlenecks for real-world implementation. Despite considerable progress, the lack of standardized performance metrics remains a major obstacle to meaningful comparison and advancement in the field. Two-terminal PBs and PSCs operate under intertwined photoelectrochemical and electrostatic mechanisms, rendering conventional figures of merit—such as photoconversion efficiency, specific capacitance, or Coulombic efficiency—insufficient to fully describe their coupled behavior. Establishing unified testing protocols that define illumination intensity, spectral range, cycling conditions, and light/dark response parameters is essential for consistent evaluation. Moreover, incorporating *in situ* and *operando* characterization techniques, including spectroelectrochemistry, time-resolved photoluminescence, and impedance spectroscopy, will be critical to decouple photogenerated and

electrochemical contributions and to elucidate charge transport pathways with higher accuracy.

Looking ahead, the development of compact photostorage systems is expected to benefit from multidisciplinary convergence between materials science, device physics, and scalable manufacturing. The implementation of lead-free perovskite-inspired materials, earth-abundant transition-metal oxides and chalcogenides, and conjugated organic frameworks [168, 169] offers a starting point for the exploration of new photoactive materials and fine-tuning of interfaces. The discovery of new multifunctional materials, combined with the investigation of emerging synthetic strategies, such as solution-based printing [170], atomic layer deposition [171], and high-throughput combinatorial screening, offers a sustainable pathway to high-performance, nontoxic devices. Further progress will rely on integrating computational materials design and machine learning approaches to predict optimal material combinations and interfacial geometries that minimize recombination and maximize energy throughput. Another promising avenue is the development of flexible and transparent device architectures, enabling integration into wearable electronics, building-integrated photovoltaics, and indoor energy-harvesting systems [158, 172, 173]. The use of photoactive solid-state or polymer-gel electrolytes will be central to achieving safe, stable, and bendable energy-storage platforms [174]. In parallel, scalability and reproducibility will determine the transition of two-terminal PBs and PSCs from laboratory prototypes to practical technologies. Advances in printing and roll-to-roll fabrication, combined with standardized benchmarking and lifecycle assessment, could pave the way toward real-world applications. In the longer term, hybrid architectures capable of multi-source harvesting, for instance combining light, thermal, or mechanical inputs, may lead to truly autonomous energy modules.

Ultimately, the continued convergence of innovative materials, device engineering, and standardized evaluation frameworks will be key to realizing robust, efficient, and multifunctional photo-rechargeable systems. By addressing the challenges of stability, spectral utilization, and reproducibility, two-terminal PBs and PSCs could mature into practical, self-sustaining power solutions for future flexible, transparent, and autonomous electronic technologies.

Acknowledgments

This work was supported by the European Research Council (EIC) through the Pathfinder Open project LEAF (ID 101186701). A.M. acknowledges financial support of Agenzia Spaziale Italiana (ASI). L.C. and T.G. thank the Deutsche Forschungsgemeinschaft (DFG) for project 514772236. A.R. was supported by the European Union – NextGenerationEU, under the Italian National Recovery and Resilience Plan (NRRP), Mission 4 Component 2 Investment 1.2, funding scheme “Young Researchers” (D.D. 201 del 3.7.2024), in the framework of the Project PEROVSKAP, SOE_2024000032.

Open access publishing facilitated by Politecnico di Torino, as part of the Wiley - CRUI-CARE agreement.

Funding

This work was supported by the HORIZON EUROPE European Innovation Council (101186701).

Conflicts of Interest

The authors declare no conflicts of interest.

Data Availability Statement

The data that support the findings of this study are available from the corresponding author upon reasonable request.

References

1. T. Miyasaka and T. N. Murakami, “The Photocapacitor: An Efficient Self-Charging Capacitor for Direct Storage of Solar Energy,” *Applied Physics Letters* 85 (2004): 3932–3934, <https://doi.org/10.1063/1.1810630>.
2. N. I. Jalal, R. I. Ibrahim, and M. K. Oudah, “A Review on Supercapacitors: Types and Components,” *Journal of Physics: Conference Series* 1973 (2021): 012015, <https://doi.org/10.1088/1742-6596/1973/1/012015>.
3. D. Schmidt, M. D. Hager, U. S. Schubert, D. Schmidt, M. D. Hager, and U. S. Schubert, “Photo-Rechargeable Electric Energy Storage Systems,” *Advanced Energy Materials* 6 (2016): 1500369, <https://doi.org/10.1002/AENM.201500369>.
4. K. S. Poonam, A. Arora, and S. K. Tripathi, “Review of Supercapacitors: Materials and Devices,” *Journal of Energy Storage* 21 (2019): 801–825, <https://doi.org/10.1016/J.EST.2019.01.010>.
5. A. Pujari, K. Shimokawa, and M. De Volder, “Photobatteries: Prospects and Fundamental Limitations,” *Joule* 9 (2025): 101869, <https://doi.org/10.1016/J.JOULE.2025.101869>.
6. S. Kansal, S. Priya, S. Porwal, A. Chandra, and T. Singh, “Integrated Energy Generation and Storage Systems for Low-Power Device Applications,” *Energy Storage* 5 (2023): e413, <https://doi.org/10.1002/EST2.413>.
7. L. Fagiolari, M. Sampò, A. Lamberti, et al., “Integrated Energy Conversion and Storage Devices: Interfacing Solar Cells, Batteries and Supercapacitors,” *Energy Storage Materials* 51 (2022): 400–434, <https://doi.org/10.1016/J.ENSM.2022.06.051>.
8. Q. Zeng, Y. Lai, L. Jiang, et al., “Integrated Photorechargeable Energy Storage System: Next-Generation Power Source Driving the Future,” *Advanced Energy Materials* 10 (2020): 1903930, <https://doi.org/10.1002/AENM.201903930>.
9. S. Domenici, R. Speranza, F. Bella, A. Lamberti, and T. Gatti, “A Sustainable Hydrogel-Based Dye-Sensitized Solar Cell Coupled to an Integrated Supercapacitor for Direct Indoor Light-Energy Storage,” *Solar RRL* 9 (2025): 2400838, <https://doi.org/10.1002/SOLR.202400838>.
10. T. Kumar, M. Kumar, A. Kumar, R. Kumar, and M. Bag, “A Review of Current Progress in Perovskite-Based Energy Storage to Photorechargeable Systems,” *Energy and Fuels* 39 (2025): 9185–9231, <https://doi.org/10.1021/ACS.ENERGYFUELS.4C05865>.
11. X. Zhang, W. L. Song, J. Tu, J. Wang, M. Wang, and S. Jiao, “A Review of Integrated Systems Based on Perovskite Solar Cells and Energy Storage Units: Fundamental, Progresses, Challenges, and Perspectives,” *Advanced Science* 8 (2021): 2100552, <https://doi.org/10.1002/ADVS.202100552>.
12. X. Xu, S. Li, H. Zhang, et al., “A Power Pack Based on Organometallic Perovskite Solar Cell and Supercapacitor,” *ACS Nano* 9 (2015): 1782–1787, <https://doi.org/10.1021/NN506651M>.
13. Y. Zhong, X. Xia, W. Mai, et al., “Integration of Energy Harvesting and Electrochemical Storage Devices,” *Advanced Materials Technologies* 2 (2017): 1700182, <https://doi.org/10.1002/ADMT.201700182>.
14. J. Lv, J. Xie, A. G. A. Mohamed, X. Zhang, and Y. Wang, “Photoelectrochemical Energy Storage Materials: Design Principles and Functional Devices towards Direct Solar to Electrochemical Energy Storage,” *Chemical Society Reviews* 51 (2022): 1511–1528, <https://doi.org/10.1039/D1CS00859E>.

15. N. Sankir and M. Sankir, *Solar Capacitors and Batteries*, accessed October 25, 2025, https://books.google.com/books?hl=it&lr=&id=1AeNEQAAQBAJ&oi=fnd&pg=PR15&dq=solar+capacitors+and+battery+sankir+2025&ots=cqexkanhQD&sig=T_JwrdAMSwKEixqIqy8n-QO7MLQ.
16. M. Yang, D. Wang, Y. Ling, X. Guo, and W. Chen, "Emerging Advanced Photo-Rechargeable Batteries," *Advanced Functional Materials* 34 (2024): 2410398, <https://doi.org/10.1002/ADFM.202410398>.
17. D. Schmidt, M. D. Hager, U. S. Schubert, D. Schmidt, M. D. Hager, and U. S. Schubert, "Photobatteries and Photocapacitors," *Springer* 6 (2016), <https://doi.org/10.1002/AENM.201500369>.
18. T. Li, Y. Zhang, L. Li, et al., "Advances on Emerging Integrated Photocapacitors: Strategies, Design, and Challenges," *Small* 21 (2025): 2504555, <https://doi.org/10.1002/SMLL.202504555>.
19. K. Liang, L. Li, and Y. Yang, "Inorganic Porous Films for Renewable Energy Storage," *ACS Energy Letters* 2 (2017): 373–390, <https://doi.org/10.1021/ACSENERGYLETT.6B00666>.
20. S. Prosandeev, D. Wang, A. R. Akbarzadeh, et al., "Inorganic Dielectric Materials for Energy Storage Applications: A Review," *Journal of Physics D: Applied Physics* 55 (2022): 183002, <https://doi.org/10.1088/1361-6463/AC46ED>.
21. B. D. Boruah, B. Wen, and M. De Volder, "Light Rechargeable Lithium-Ion Batteries Using V₂O₅ Cathodes," *Nano Letters* 21 (2021): 3527–3532, <https://doi.org/10.1021/ACS.NANOLETT.1C00298>.
22. I. Ciria-Ramos, E. J. Juarez-Perez, M. Haro, et al., "Solar Energy Storage Using a Cu₂O-TiO₂ Photocathode in a Lithium Battery," *Small* 19 (2023): 2301244, <https://doi.org/10.1002/SMLL.202301244>.
23. R. Khatoon, M. Nazir, R. T. Baker, et al., "Breaking the Capacity Limit for WO₃ Anode-Based Li-Ion Batteries Using Photo-Assisted Charging," *Advanced Functional Materials* 35 (2025): 2501498, <https://doi.org/10.1002/ADFM.202501498>.
24. I. K. Popoola, M. A. Gondal, A. J. Popoola, L. E. Oloore, and M. Younas, "Inorganic Perovskite Photo-Assisted Supercapacitor for Single Device Energy Harvesting and Storage Applications," *Journal of Energy Storage* 73 (2023): 108828, <https://doi.org/10.1016/J.EST.2023.108828>.
25. T. Li, X. Chen, K. Ren, et al., "Dual-Electric-Field Synergy in CdS/NiCo₂S₄ Heterojunctions for Flexible Integrated Photo-Supercapacitors," *Chemical Engineering Journal* 520 (2025): 166290, <https://doi.org/10.1016/J.CEJ.2025.166290>.
26. A. S. Renani, Z. Hosseini, D. Eberhart, A. W. Maijenburg, and M. M. Momeni, "Photo-Assisted Symmetric and Asymmetric Supercapacitors Based on Molybdenum Cobalt Coated Bismuth Vanadate Photoelectrodes: All-in-One Energy Harvesting and Storage Devices," *Journal of Power Sources* 640 (2025): 236687, <https://doi.org/10.1016/J.JPOWSOUR.2025.236687>.
27. M. M. Momeni, Z. Yazdani, and H. M. Aydisheh, "Light-Assisted Supercapacitors Based on CNT-WO₃ Hybrid Dual Photoelectrodes," *Journal of Alloys and Compounds* 1031 (2025): 180973, <https://doi.org/10.1016/J.JALLCOM.2025.180973>.
28. M. M. Momeni, A. S. Renani, and B. K. Lee, "Light-Chargeable Two-Electrode Photo-Supercapacitors Based on MnS Nanoflowers Deposited on V₂O₅-BiVO₄ Photoelectrodes," *Journal of Alloys and Compounds* 962 (2023): 171204, <https://doi.org/10.1016/J.JALLCOM.2023.171204>.
29. X. Liu, H. Andersen, Y. Lu, et al., "Porous Carbon Coated on Cadmium Sulfide-Decorated Zinc Oxide Nanorod Photocathodes for Photo-Accelerated Zinc Ion Capacitors," *ACS Applied Materials & Interfaces* 15 (2023): 6963–6969, <https://doi.org/10.1021/ACSAMI.2C20995>.
30. X. Ma, J. Fu, L. Gao, et al., "Dual-Duty NiCo₂S₄ Nanosheet-Based Solar Rechargeable Batteries toward Multi-Scene Solar Energy Conversion and Storage," *Nanoscale* 15 (2023): 10584–10592, <https://doi.org/10.1039/D3NR01483E>.
31. M. Najafi and M. M. Momeni, "Flexible Photo-Assisted Supercapacitor Utilizing Ternary Mn-Ni-Co Sulfides on Titania Electrodes," *Chemical Engineering Journal* 507 (2025): 160555, <https://doi.org/10.1016/J.CEJ.2025.160555>.
32. D. Yang, X. Li, and H. Zeng, "Surface Chemistry of All Inorganic Halide Perovskite Nanocrystals: Passivation Mechanism and Stability," *Advanced Materials Interfaces* 5 (2018): 1701662, <https://doi.org/10.1002/ADMI.201701662>.
33. C. Chesta, J. Subbiah, D. J. Jones, and S. Srinivasan, "Sampath Srinivasan, Efficient Photo-Rechargeable Aqueous Zinc-Ion Batteries Using Lead-Free Perovskite Photocathodes," *Journal of Materials Chemistry A* (2025), <https://doi.org/10.1039/D5TA05014F>.
34. S. K. Bhaumik, S. Biswas, N. Shauloff, et al., "Photo-Rechargeable Organic Supercapacitor via Light-Activated Electrolytes," *Advanced Science* 12 (2025): 2500978, <https://doi.org/10.1002/ADVS.202500978>.
35. X. Zhang, Y. Gao, J. C. Jiao, Z. H. Wang, L. B. Gao, and G. Y. Zhang, "Fashioned Performance-Boosting On-Chip Planar Microsupercapacitors Based on Chemical Vapor Deposition Graphene and Graphene Quantum Dot Heterostructures," *ACS Applied Nano Materials* 8 (2025): 15255–15267, <https://doi.org/10.1021/ACSANM.5C02580>.
36. A. Gouder, F. Podjaski, A. Jiménez-Solano, J. Kröger, Y. Wang, and B. V. Lotsch, "An Integrated Solar Battery Based on a Charge Storing 2D Carbon Nitride," *Energy & Environmental Science* 16 (2023): 1520–1530, <https://doi.org/10.1039/D2EE03409C>.
37. K. Surana, D. B. Kanani, S. N. Bariya, et al., "Unconventional Photocapacitor Utilizing Metal-Organic Dye Capable of Operating in Low Intensity Light," *ACS Applied Materials & Interfaces* 17 (2025): 7938–7947, <https://doi.org/10.1021/ACSAMI.4C15730>.
38. K. Kato, A. B. Puthirath, A. Mojiypour, et al., "Light-Assisted Rechargeable Lithium Batteries: Organic Molecules for Simultaneous Energy Harvesting and Storage," *Nano Letters* 21 (2021): 907–913.
39. N. Flores-Diaz, F. De Rossi, T. Keller, et al., "Unlocking High-Performance Photocapacitors for Edge Computing in Low-Light Environments," *Energy & Environmental Science* 18 (2025): 4704–4716, <https://doi.org/10.1039/D5EE01052G>.
40. Z. Yang, L. Li, Y. Luo, et al., "An Integrated Device for Both Photoelectric Conversion and Energy Storage Based on Free-Standing and Aligned Carbon Nanotube Film," *Journal of Materials Chemistry A* 1 (2013): 954–958, <https://doi.org/10.1039/C2TA00113F>.
41. K. Liu, Z. Chen, T. Lv, et al., "A Self-Supported Graphene/Carbon Nanotube Hollow Fiber for Integrated Energy Conversion and Storage," *Nano-Micro Letters* 12 (2020): 1–11, <https://doi.org/10.1007/S40820-020-0390-X>.
42. J. Li, K. Zhang, Y. Zhao, et al., "High-Efficiency and Stable Li–CO₂ Battery Enabled by Carbon Nanotube/Carbon Nitride Heterostructured Photocathode," *Angewandte Chemie International Edition* 61 (2022): e202114612, <https://doi.org/10.1002/ANIE.202114612>.
43. W. Wang, X. Zhang, J. Lin, et al., "A Photoresponsive Battery Based on a Redox-Coupled Covalent-Organic-Framework Hybrid Photoelectrochemical Cathode," *Angewandte Chemie International Edition* 61 (2022): e202214816, <https://doi.org/10.1002/ANIE.202214816>.
44. G. Qu, J. Cheng, X. Li, et al., "A Fiber Supercapacitor with High Energy Density Based on Hollow Graphene/Conducting Polymer Fiber Electrode," *Advanced Materials* 28 (2016): 3646–3652, <https://doi.org/10.1002/ADMA.201600689>.
45. P. Dong, M. T. F. Rodrigues, J. Zhang, et al., "A Flexible Solar Cell/Supercapacitor Integrated Energy Device," *Nano Energy* 42 (2017): 181–186, <https://doi.org/10.1016/J.NANOEN.2017.10.035>.
46. S. Ramandi and M. H. Entezari, "FeCo₂O₄@Bi₂S₃ S-Scheme Heterojunction for Photo-Rechargeable Zn-Ion Capacitors," *Chemical Engineering Journal* 520 (2025): 166373, <https://doi.org/10.1016/J.CEJ.2025.166373>.

47. A. Mozafari, M. M. Momeni, A. Naderi, and B. K. Lee, "Photo-Rechargeable Zinc Ion Capacitors Using $\text{MoS}_2/\text{NaTaO}_3/\text{CF}$ Dual-Acting Electrodes Prepared by Photodeposition Method," *Nanoscale* 17 (2025): 919–933, <https://doi.org/10.1039/D4NR03936J>.
48. Y. K. Liu, C. Z. Zhao, J. Du, X. Q. Zhang, A. B. Chen, and Q. Zhang, "Research Progresses of Liquid Electrolytes in Lithium-Ion Batteries," *Small* 19 (2023): 2205315, <https://doi.org/10.1002/SMLL.202205315>.
49. A. Mendhe and H. S. Panda, "A Review on Electrolytes for Supercapacitor Device," *Discover Materials* 3 (2023): 1–27, <https://doi.org/10.1007/S43939-023-00065-3>.
50. P. S. Chauhan, M. Parekh, S. Sahoo, et al., "Influence of Electrolyte on the Photo-Charging Capability of a ZnO–FTO Supercapacitor," *Journal of Materials Chemistry A* 12 (2024): 22725–22736, <https://doi.org/10.1039/D4TA04702H>.
51. Z. Pan, L. Yao, J. Zhai, X. Yao, and H. Chen, "Interfacial Coupling Effect in Organic/Inorganic Nanocomposites with High Energy Density," *Advanced Materials* 30 (2018): 1705662, <https://doi.org/10.1002/ADMA.201705662>.
52. N. Gao and X. Fang, "Synthesis and Development of Graphene–Inorganic Semiconductor Nanocomposites," *Chemical Reviews* 115 (2015): 8294–8343, <https://doi.org/10.1021/CR400607Y>.
53. N. Tewari, S. B. Shivarudraiah, and J. E. Halpert, "Photorechargeable Lead-Free Perovskite Lithium-Ion Batteries Using Hexagonal $\text{Cs}_3\text{Bi}_2\text{I}_9$ Nanosheets," *Nano Letters* 21 (2021): 5578–5585, <https://doi.org/10.1021/ACS.NANOLETT.1C01000>.
54. N. Eswaramoorthy, S. Rajendran, B. A. Kumar, et al., "Influence of ZnO/MWCNTs Based Hybrid Electrodes for Boosting the Performance of Photovoltaic and Supercapacitor Devices," *Materials Chemistry and Physics* 316 (2024): 129049, <https://doi.org/10.1016/J.MATCHEMPHYS.2024.129049>.
55. R. Zhang, Z. Chen, X. Li, et al., "Dual-Functional $\text{Cs}_3\text{Bi}_2\text{Br}_9$ for Stable All-Solid-State Photo-Rechargeable Batteries," *Journal of Power Sources* 624 (2024): 235530, <https://doi.org/10.1016/J.JPOWSOUR.2024.235530>.
56. Y. Zhai, Y. Dou, D. Zhao, P. F. Fulvio, R. T. Mayes, and S. Dai, "Carbon Materials for Chemical Capacitive Energy Storage," *Advanced Materials* 23 (2011): 4828–4850, <https://doi.org/10.1002/ADMA.201100984>.
57. D. K. Kampouris, X. Ji, E. P. Randviir, and C. E. Banks, "A New Approach for the Improved Interpretation of Capacitance Measurements for Materials Utilised in Energy Storage," *RSC Advances* 5 (2015): 12782–12791, <https://doi.org/10.1039/C4RA17132B>.
58. C. Choi, D. S. Ashby, D. M. Butts, et al., "Achieving High Energy Density and High Power Density with Pseudocapacitive Materials," *Nature Reviews Materials* 5 (2020): 5–19, <https://doi.org/10.1038/S41578-019-0142-Z>.
59. Y. Gogotsi and P. Simon, "True Performance Metrics in Electrochemical Energy Storage," *Science* 334 (2011): 917–918, <https://doi.org/10.1126/SCIENCE.1213003>.
60. Z. Zhang, X. Chen, P. Chen, et al., "Integrated Polymer Solar Cell and Electrochemical Supercapacitor in a Flexible and Stable Fiber Format," *Advanced Materials* 26 (2013): 466, <https://doi.org/10.1002/adma.201302951>.
61. L. Rebecchi, I. Martin, I. M. Albo, et al., "Scalable Production of Metal Oxide Nanoparticles for Optoelectronics Applications," *Chemistry: A European Journal* 31 (2025): e202401711, <https://doi.org/10.1002/CHEM.202401711>.
62. M. Ghini, N. Curreli, A. Camellini, M. Wang, A. Asaithambi, and I. Kriegel, "Photodoping of Metal Oxide Nanocrystals for Multi-Charge Accumulation and Light-Driven Energy Storage," *Nanoscale* 13 (2021): 8773–8783, <https://doi.org/10.1039/D0NR09163D>.
63. C. K. Brozek, D. Zhou, H. Liu, X. Li, K. R. Kittilstved, and D. R. Gamelin, "Soluble Supercapacitors: Large and Reversible Charge Storage in Colloidal Iron-Doped ZnO Nanocrystals," *Nano Letters* 18 (2018): 3297–3302, <https://doi.org/10.1021/acs.nanolett.8b01264>.
64. I. Kriegel, C. Urso, D. Viola, et al., "Ultrafast Photodoping and Plasmon Dynamics in Fluorine–Indium Codoped Cadmium Oxide Nanocrystals for All-Optical Signal Manipulation at Optical Communication Wavelengths," *Journal of Physical Chemistry Letters* 7 (2016): 3873–3881, <https://doi.org/10.1021/ACS.JPCLETT.6B01904>.
65. R. Eglitis, U. Joost, A. Zukuls, et al., "Strong, Rapid, and Reversible Photochromic Response of Nb Doped TiO_2 Nanocrystal Colloids in Hole Scavenging Media," *ACS Applied Materials & Interfaces* 12 (2020): 57609–57618, <https://doi.org/10.1021/ACSAMI.0C17902>.
66. M. Abdullah, R. J. Nelson, and K. R. Kittilstved, "Sub-Bandgap Trap Sites for High-Density Photochemical Electron Storage in Colloidal SrTiO_3 Nanocrystals," *Chemical Communications* 58 (2022): 11835–11838, <https://doi.org/10.1039/D2CC04328A>.
67. M. Ghini, A. Rubino, A. Camellini, and I. Kriegel, "Multi-Charge Transfer from Photodoped ITO Nanocrystals," *Nanoscale Advances* 3 (2021): 6628–6634, <https://doi.org/10.1039/D1NA00656H>.
68. A. W. Cohn, N. Janßen, J. M. Mayer, and D. R. Gamelin, "Photocharging ZnO Nanocrystals: Picosecond Hole Capture, Electron Accumulation, and Auger Recombination," *Journal of Physical Chemistry C* 116 (2012): 20633–20642, <https://doi.org/10.1021/JP3075942>.
69. K. E. Shulenberger, H. R. Keller, L. M. Pellows, N. L. Brown, and G. Dukovic, "Photocharging of Colloidal CdS Nanocrystals," *The Journal of Physical Chemistry C* 125 (2021): 22650–22659, <https://doi.org/10.1021/ACS.JPCC.1C06491>.
70. B. Bueken, F. Vermoortele, D. E. P. Vanpoucke, et al., "A Flexible Photoactive Titanium Metal–Organic Framework Based on a $[\text{Ti}^{\text{IV}}_3(\mu_3\text{-O})(\text{O})_2(\text{COO})_6]$ Cluster," *Angewandte Chemie International Edition* 54 (2015): 13912–13917, <https://doi.org/10.1002/ANIE.201505512>.
71. S. Amthor, S. Knoll, M. Heiland, et al., "A Photosensitizer–polyoxometalate Dyad that Enables the Decoupling of Light and Dark Reactions for Delayed on-Demand Solar Hydrogen Production," *Nature Chemistry* 14, no. 3 (2022): 321–327, <https://doi.org/10.1038/s41557-021-00850-8> 2022.
72. B. Matt, J. Fize, J. Moussa, et al., "Charge Photo-Accumulation and Photocatalytic Hydrogen Evolution under Visible Light at an Iridium(III)-Photosensitized Polyoxotungstate," *Energy & Environmental Science* 6 (2013): 1504–1508, <https://doi.org/10.1039/C3EE40352A>.
73. V. W.-hei Lau, D. Klose, H. Kasap, et al., "Dark Photocatalysis: Storage of Solar Energy in Carbon Nitride for Time-Delayed Hydrogen Generation," *Angewandte Chemie* 129 (2017): 525–529, <https://doi.org/10.1002/ANGE.201608553>.
74. Z. Chen, A. Savateev, S. Pronkin, et al., "The Easier the Better" Preparation of Efficient Photocatalysts—Metastable Poly(heptazine Imide) Salts," *Advanced Materials* 29 (2017): 1700555, <https://doi.org/10.1002/ADMA.201700555>.
75. M. M. Miller and A. A. Lazarides, "Sensitivity of Metal Nanoparticle Surface Plasmon Resonance to the Dielectric Environment," *Journal of Physical Chemistry B* 109 (2005): 21556–21565, <https://doi.org/10.1021/JP054227Y>.
76. L. Rebecchi, N. Petrini, I. M. Albo, N. Curreli, and A. Rubino, "Transparent Conducting Metal Oxides Nanoparticles for Solution-Processed Thin Films Optoelectronics," *Optical Materials: X* 19 (2023): 100247, <https://doi.org/10.1016/J.OMX.2023.100247>.
77. S. Sahoo, K. Y. Wickramathilaka, E. Njeri, D. Silva, and S. L. Suib, "A Review on Transition Metal Oxides in Catalysis," *Frontiers in Chemistry* 12 (2024): 1374878, <https://doi.org/10.3389/FCHEM.2024.1374878/FULL>.
78. D. Astruc, "Transition-Metal Nanoparticles in Catalysis: From Historical Background to the State-of-the Art," *Nanoparticles and Catalysis* (2008): 1–48, <https://doi.org/10.1002/9783527621323.CH1>.

79. N. Flores-Diaz, F. De Rossi, A. Das, M. Deepa, F. Brunetti, and M. Freitag, "Progress of Photocapacitors," *Chemical Reviews* 123 (2023): 9327–9355, <https://doi.org/10.1021/ACS.CHEMREV.2C00773>.
80. S. Kumar, S. Saralch, U. Jabeen, and D. Pathak, "Metal Oxides for Energy Applications," in *Colloidal Metal Oxide Nanoparticles* (Elsevier, 2020), 471–504, <https://doi.org/10.1016/B978-0-12-813357-6.00017-6>.
81. X. Xia, Y. Zhang, D. Chao, et al., "Solution Synthesis of Metal Oxides for Electrochemical Energy Storage Applications," *Nanoscale* 6 (2014): 5008–5048, <https://doi.org/10.1039/C4NR00024B>.
82. A. Karatutlu, A. Barhoum, and A. Sapelkin, "Liquid-Phase Synthesis of Nanoparticles and Nanostructured Materials," in *Emerging Applications of Nanoparticles and Architectural Nanostructures: Current Prospects and Future Trends* (Elsevier, 2018): 1–28, <https://doi.org/10.1016/B978-0-323-51254-1.00001-4>.
83. H. Zheng, J. Z. Ou, M. S. Strano, R. B. Kaner, A. Mitchell, and K. Kalantar-Zadeh, "Nanostructured Tungsten Oxide - Properties, Synthesis, and Applications," *Advanced Functional Materials* 21 (2011): 2175–2196, <https://doi.org/10.1002/ADFM.201002477>.
84. A. K. Lichchhavi and P. M. Shirage, "A Review on Synergy of Transition Metal Oxide Nanostructured Materials: Effective and Coherent Choice for Supercapacitor Electrodes," *Journal of Energy Storage* 55 (2022): 105692, <https://doi.org/10.1016/J.EST.2022.105692>.
85. J. Gong, J. Liang, and K. Sumathy, "Review on Dye-Sensitized Solar Cells (DSSCs): Fundamental Concepts and Novel Materials," *Renewable and Sustainable Energy Reviews* 16 (2012): 5848–5860, <https://doi.org/10.1016/J.RSER.2012.04.044>.
86. J. Gong, K. Sumathy, Q. Qiao, and Z. Zhou, "Review on Dye-Sensitized Solar Cells (DSSCs): Advanced Techniques and Research Trends," *Renewable and Sustainable Energy Reviews* 68 (2017): 234–246, <https://doi.org/10.1016/J.RSER.2016.09.097>.
87. K. Sharma, V. Sharma, and S. S. Sharma, "Dye-Sensitized Solar Cells: Fundamentals and Current Status," *Nanoscale Research Letters* 13 (2018): 1–46, <https://doi.org/10.1186/S11671-018-2760-6>.
88. A. Omar, M. S. Ali, and N. Abd Rahim, "Electron Transport Properties Analysis of Titanium Dioxide Dye-Sensitized Solar Cells (TiO₂-DSSCs) Based Natural Dyes Using Electrochemical Impedance Spectroscopy Concept: A Review," *Solar Energy* 207 (2020): 1088–1121, <https://doi.org/10.1016/J.SOLENER.2020.07.028>.
89. Z. S. Wang, H. Kawauchi, T. Kashima, and H. Arakawa, "Significant Influence of TiO₂ Photoelectrode Morphology on the Energy Conversion Efficiency of N719 Dye-Sensitized Solar Cell," *Coordination Chemistry Reviews* 248 (2004): 1381–1389, <https://doi.org/10.1016/J.CCR.2004.03.006>.
90. T. Raguram and K. S. Rajni, "Effect of Ni Doping on the Characterization of TiO₂ Nanoparticles for DSSC Applications," *Journal of Materials Science: Materials in Electronics* 32 (2021): 18264–18281, <https://doi.org/10.1007/S10854-021-06369-5>.
91. T. Sakthivel, K. A. Kumar, J. Senthilselvan, and K. Jagannathan, "Effect of Ni Dopant in TiO₂ Matrix on Its Interfacial Charge Transportation and Efficiency of DSSCs," *Journal of Materials Science: Materials in Electronics* 29 (2018): 2228–2235, <https://doi.org/10.1007/S10854-017-8137-2>.
92. Y. Zhang, H. Tao, H. Wang, J. Hao, Y. Liu, and Y. Yuan, "Sol-Gel Synthesis of Magnesium Doped TiO₂ Thin Film and Its Application in Dye Sensitized Solar Cell," *Optical Materials* 158 (2025): 116446, <https://doi.org/10.1016/J.OPTMAT.2024.116446>.
93. R. Speranza, M. Reina, P. Zaccagnini, A. Pedico, and A. Lamberti, "Laser-Induced Graphene as a Sustainable Counter Electrode for DSSC Enabling Flexible Self-Powered Integrated Harvesting and Storage Device for Indoor Application," *Electrochimica Acta* 460 (2023): 142614, <https://doi.org/10.1016/J.ELECTACTA.2023.142614>.
94. J. K. Davis, J. George, and M. Balachandran, "Integrating Dye-Sensitized Solar Cells and Supercapacitors: Portable Powerpacks for Future Energy Applications," *Journal of Materials Science* 59 (2024): 20176–20203, <https://doi.org/10.1007/S10853-024-10344-W>.
95. B. D. Boruah, B. Wen, S. Nagane, et al., "Photo-Rechargeable Zinc-Ion Capacitors Using V₂O₅-Activated Carbon Electrodes," *ACS Energy Letters* 5 (2020): 3132–3139, <https://doi.org/10.1021/ACSENERGYLETT.0C01528>.
96. J. Banerjee, N. Rashmi, G. P. Sharma, A. Nagendra, D. Bhattacharyya, and S. Sivakumar, "Vanadium Doping Enhances the Photo-Capacity of Fe₂O₃ Nanoflowers: A Promising Photo-Electrode for Aqueous Iron Ion Photo-Capacitors," *Sustainable Energy & Fuels* 9 (2025): 4451–4470, <https://doi.org/10.1039/D5SE00037H>.
97. G. B. Yildirim and E. Daş, "The Synthesis of MgO and MgO-Graphene Nanocomposite Materials and Their Diode and Photodiode Applications," *Physica Scripta* 98 (2023): 085911, <https://doi.org/10.1088/1402-4896/ACE249>.
98. S. S. Patil, A. G. Bhosale, Y. V. Ambole, et al., "Unveiling Light-Modulated Capacitance of Sea Urchin like δ-MnO₂: A Smart Flexible Photocapacitive Device," *Journal of Energy Storage* 101 (2024): 113904, <https://doi.org/10.1016/J.EST.2024.113904>.
99. C. Lefdhil, S. Polat, and H. Zengin, "Synthesis of Zinc Oxide Nanorods from Zinc Borate Precursor and Characterization of Supercapacitor Properties," *Nanomaterials* 13 (2023): 2423, <https://doi.org/10.3390/NANO13172423>.
100. A. Mohan, V. Manikandan, S. Devanesan, et al., "Nanostructured Nickel Doped Zinc Oxide Material Suitable for Magnetic, Supercapacitor Applications and Theoretical Investigation," *Chemosphere* 299 (2022): 134366, <https://doi.org/10.1016/J.CHEMOSPHERE.2022.134366>.
101. M. Yadav, S. Choudhari, P. Kumar, and P. Ram, "Physical and Electrochemical Performance of Mn-Doped Zinc Oxide Electrode Material for Asymmetric Supercapacitor," *Journal of the Indian Chemical Society* 101 (2024): 101416, <https://doi.org/10.1016/J.JICS.2024.101416>.
102. C. T. Altaf, O. Coskun, A. Kumtepe, et al., "Photo-Supercapacitors Based on Nanoscaled ZnO," *Scientific Reports* 12 (2022): 1–15, <https://doi.org/10.1038/S41598-022-15180-Z>.
103. C. T. Altaf, T. O. Colak, A. M. Rostas, et al., "Zinc Oxide Nanoflake/Reduced Graphene Oxide Nanocomposite-Based Dual-Acting Electrodes for Solar-Assisted Supercapacitor Applications," *Energy Advances* 3 (2024): 1965–1976, <https://doi.org/10.1039/D4YA00253A>.
104. P. Saini, J. K. Yadav, B. Rani, and A. Dixit, "Light-Driven Enhancement in the Pseudocapacitance of Nanosized ZnO Particles and Carbon Nanotube-Based Photo-Rechargeable Supercapacitors," *Journal of Materials Chemistry A* 13 (2025): 25543–25558, <https://doi.org/10.1039/D5TA03620H>.
105. A. Kumar, R. Hammad, M. Pahuja, et al., "Photo-Rechargeable Li-Ion Batteries Using TiS₂ Cathode," *Small* 19 (2023): 2303319, <https://doi.org/10.1002/SMLL.202303319>.
106. J. Liang, C. Wang, Y. Wang, et al., "All-Inorganic Perovskite Solar Cells," *Journal of the American Chemical Society* 138 (2016): 15829–15832, <https://doi.org/10.1021/JACS.6B10227>.
107. N. A. N. Ouedraogo, Y. Chen, Y. Y. Xiao, et al., "Stability of All-Inorganic Perovskite Solar Cells," *Nano Energy* 67 (2020): 104249, <https://doi.org/10.1016/J.NANOEN.2019.104249>.
108. J. Duan, H. Xu, W. E. I. Sha, et al., "Inorganic Perovskite Solar Cells: An Emerging Member of the Photovoltaic Community," *Journal of Materials Chemistry A* 7 (2019): 21036–21068, <https://doi.org/10.1039/C9TA06674H>.
109. F. Schmitz, R. Bhatia, F. Lamberti, S. Meloni, and T. Gatti, "Heavy Pnictogens-Based Perovskite-Inspired Materials: Sustainable Light-Harvesters for Indoor Photovoltaics," *APL Energy* 1 (2023): 021502, <https://doi.org/10.1063/5.0161023>.

110. N. Tewari, D. Lam, P. K. Ko, et al., "Photo-Rechargeable Li-Ion Batteries with Lead-Free Double-Perovskite Halide $\text{Cs}_2\text{NaBiI}_6$," *ACS Applied Materials & Interfaces* 17 (2025): 44360–44367, <https://doi.org/10.1021/ACSAMI.5C06043>.
111. B. A., T. K., G. Ramalingam, et al., "Nanoarchitectonics of MoS_2 Petals with $\text{OD}@2\text{D}$ Carbon Derivatives for Integrated Photocapacitor Application," *Journal of Alloys and Compounds* 1010 (2025): 177622, <https://doi.org/10.1016/J.JALLCOM.2024.177622>.
112. T. Kajana, A. Pirashanthan, A. Yuvapragasam, D. Velauthapillai, P. Ravirajan, and M. Senthilnathanan, "Bimetallic $\text{AC}/\text{Ag}_2\text{CrO}_4/\text{SnS}$ Heterostructure Photoanode for Energy Conversion and Storage: A Self-Powered Photocapacitor," *Journal of Power Sources* 520 (2022): 230883, <https://doi.org/10.1016/J.JPOWSOUR.2021.230883>.
113. C. Cui, X. Wang, H. Zhu, et al., "Photo-Assisted Enhancement of Lithium-Ion Battery Performance with a $\text{LiFePO}_4/\text{TiO}_2$ Composite Cathode," *Ceramics International* 50 (2024): 11291–11297, <https://doi.org/10.1016/J.CERAMINT.2024.01.029>.
114. S. M. Benoy, M. Pandey, D. Bhattacharjya, and B. K. Saikia, "Recent Trends in Supercapacitor-Battery Hybrid Energy Storage Devices Based on Carbon Materials," *Journal of Energy Storage* 52 (2022): 104938, <https://doi.org/10.1016/J.EST.2022.104938>.
115. S. Iqbal, H. Khatoun, A. Hussain Pandit, and S. Ahmad, "Recent Development of Carbon Based Materials for Energy Storage Devices," *Materials Science for Energy Technologies* 2 (2019): 417–428, <https://doi.org/10.1016/J.MSET.2019.04.006>.
116. L. Wang, L. Wen, Y. Tong, et al., "Photo-Rechargeable Batteries and Supercapacitors: Critical Roles of Carbon-Based Functional Materials," *Carbon Energy* 3 (2021): 225–252, <https://doi.org/10.1002/CEY2.105>.
117. M. Alexandri, C. B. Brocchi, D. M. Soares, et al., "Pseudocapacitive Behaviour of Iron Oxides Supported on Carbon Nanofibers as a Composite Electrode Material for Aqueous-Based Supercapacitors," *Journal of Energy Storage* 42 (2021): 103052, <https://doi.org/10.1016/J.EST.2021.103052>.
118. M. Heydari Gharahcheshmeh and K. Chowdhury, "Fabrication Methods, Pseudocapacitance Characteristics, and Integration of Conjugated Conducting Polymers in Electrochemical Energy Storage Devices," *Energy Advances* 3 (2024): 2668–2703, <https://doi.org/10.1039/D4YA00504J>.
119. E. E. Miller, Y. Hua, and F. H. Tezel, "Materials for Energy Storage: Review of Electrode Materials and Methods of Increasing Capacitance for Supercapacitors," *Journal of Energy Storage* 20 (2018): 30–40, <https://doi.org/10.1016/J.EST.2018.08.009>.
120. K. Tang, J. Chang, H. Cao, et al., "Macropore- and Micropore-Dominated Carbon Derived from Poly(vinyl Alcohol) and Polyvinylpyrrolidone for Supercapacitor and Capacitive Deionization," *ACS Sustainable Chemistry & Engineering* 5 (2017): 11324–11333, <https://doi.org/10.1021/ACSSUSCHEMENG.7B02307>.
121. Z. Supiyeva, X. Pan, and Q. Abbas, "The Critical Role of Nanostructured Carbon Pores in Supercapacitors," *Current Opinion in Electrochemistry* 39 (2023): 101249, <https://doi.org/10.1016/J.COELEC.2023.101249>.
122. J. Melke, J. Martin, M. Bruns, et al., "Investigating the Effect of Microstructure and Surface Functionalization of Mesoporous N-Doped Carbons on $\text{V}^{4+}/\text{V}^{5+}$ Kinetics," *ACS Applied Energy Materials* 3 (2020): 11627, <https://doi.org/10.1021/ACSAEM.0C01489>.
123. T. N. Murakami, N. Kawashima, and T. Miyasaka, "A High-Voltage Dye-Sensitized Photocapacitor of a Three-Electrode System," *Chemical Communications* (2005): 3346–3348, <https://doi.org/10.1039/B503122B>.
124. J. Vigneshwaran, S. Abraham, Y. K. Vasudevan, T. Prasankumar, S. P. Jose, and J. Jose, "Carbon Nanotube-Based Nanostructured Materials for Supercapacitor Applications: Synthesis and Electrochemical Analysis, *Nanostructured Materials for Energy Storage I-IV*," (2024): 1011–1059, <https://doi.org/10.1002/9783527838851.CH28>.
125. E. Frackowiak and F. Beguin, *Carbon Materials for the Electrochemical Storage of Energy in Capacitors* (2001).
126. C. Du and N. Pan, "Supercapacitors Using Carbon Nanotubes Films by Electrophoretic Deposition," *Journal of Power Sources* 160, no. 2 (2006): 1487–1494, <https://doi.org/10.1016/J.JPOWSOUR.2006.02.092>.
127. S. Ahmad, C. George, D. J. Beesley, J. J. Baumberg, and M. De Volder, "Photo-Rechargeable Organo-Halide Perovskite Batteries," *Nano Letters* 18 (2018): 1856–1862, <https://doi.org/10.1021/ACS.NANOLETT.7B05153>.
128. B. Arjun Kumar, V. A.F.Samson, F. Ran, P. S. Maram, and S. Sangaraju, "Progressive Horizons of Energy Generation and Storage: Nook and Cranny of Photo-Supercapacitors," *Journal of Energy Storage* 97 (2024): 112876, <https://doi.org/10.1016/J.EST.2024.112876>.
129. Q. Adfar, S. Hussain, and S. S. Maktedar, "Insights into Energy and Environmental Sustainability through Photoactive Graphene-Based Advanced Materials: Perspectives and Promises," *New Journal of Chemistry* 49 (2025): 2511–2650, <https://doi.org/10.1039/D4NJ03693J>.
130. M. Manikandan, V. Anto Feradrick Samson, E. Manikandan, K. A. Karthigeyan, and E. Papanasam, "A Comprehensive Review on Materials Research Progress and Applications of Photo-Supercapacitors," *Journal of Electronic Materials* 54 (2025): 4981–5004, <https://doi.org/10.1007/S11664-025-11981-W>.
131. E. T. Mombeshora, E. Muchuweni, and P. G. Ndungu, "Applications of Graphitic Carbonaceous Materials in Photosupercapacitors: Recent Breakthroughs and Future Perspectives," *Journal of Energy Storage* 134 (2025): 118272, <https://doi.org/10.1016/J.EST.2025.118272>.
132. L. Q. Wang, "Graphene Layer Reduced Back-Transport Reaction and Increased Power Conversion Efficiency of Dye-Sensitized Solar Cells," *Materials Research Innovations* 19 (2015): S5-316–S5-319, <https://doi.org/10.1179/1432891714Z.0000000001101>.
133. B. D. Boruah, A. Mathieson, B. Wen, S. Feldmann, W. M. Dose, and M. De Volder, "Photo-Rechargeable Zinc-Ion Batteries," *Energy & Environmental Science* 13 (2020): 2414–2421, <https://doi.org/10.1039/D0EE01392G>.
134. F. Bu, W. Zhou, Y. Xu, Y. Du, C. Guan, and W. Huang, "Recent Developments of Advanced Micro-Supercapacitors: Design, Fabrication and Applications," *Npj Flexible Electronics* 4 (2020): 1–16, <https://doi.org/10.1038/S41528-020-00093-6>.
135. G. Zamiri and S. Bagheri, "Fabrication of Green Dye-Sensitized Solar Cell Based on ZnO Nanoparticles as a Photoanode and Graphene Quantum Dots as a Photo-Sensitizer," *Journal of Colloid and Interface Science* 511 (2018): 318–324, <https://doi.org/10.1016/J.JCIS.2017.10.026>.
136. W. Wu, H. Wu, M. Zhong, and S. Guo, "Dual Role of Graphene Quantum Dots in Active Layer of Inverted Bulk Heterojunction Organic Photovoltaic Devices," *ACS Omega* 4 (2019): 16159–16165, <https://doi.org/10.1021/ACSOMEGA.9B02348>.
137. Y. Liu, N. Li, S. Wu, et al., "Reducing the Charging Voltage of a Li-O_2 Battery to 1.9 V by Incorporating a Photocatalyst," *Energy & Environmental Science* 8 (2015): 2664–2667, <https://doi.org/10.1039/C5EE01958C>.
138. A. Gouder, L. Yao, Y. Wang, et al., "Bridging the Gap between Solar Cells and Batteries: Optical Design of Bifunctional Solar Batteries Based on 2D Carbon Nitrides," *Advanced Energy Materials* 13 (2023): 2300245, <https://doi.org/10.1002/AENM.202300245>.
139. S. Vadivel, "Photo-Supercapacitor," *Materials Research Foundations* 61 (2019): 223–232, <https://doi.org/10.21741/9781644900499-9>.
140. A. Sen, M. H. Putra, A. K. Biswas, A. K. Behera, and A. Groß, "Insight on the Choice of Sensitizers/Dyes for Dye Sensitized Solar Cells: A Review," *Dyes and Pigments* 213 (2023): 111087, <https://doi.org/10.1016/J.DYEPIG.2023.111087>.
141. D. Kuciauskas, J. E. Monat, R. Villahermosa, H. B. Gray, N. S. Lewis, and J. K. McCusker, "Transient Absorption Spectroscopy of Ruthenium

- and Osmium Polypyridyl Complexes Adsorbed onto Nanocrystalline TiO₂ Photoelectrodes," *Journal of Physical Chemistry B* 106 (2002): 9347–9358, <https://doi.org/10.1021/JP014589F>.
142. A. Colombo, C. Dragonetti, F. Fagnani, and D. Roberto, "Recent Developments of Ruthenium Complexes for Dye-Sensitized Solar Cells," *Electronics* 14 (2025): 1639, accessed October 25, 2025, <https://www.mdpi.com/2079-9292/14/8/1639/htm>.
143. D. Devadiga, M. Selvakumar, P. Shetty, and M. S. Santosh, "Recent Progress in Dye Sensitized Solar Cell Materials and Photo-Supercapacitors: A Review," *Journal of Power Sources* 493 (2021): 229698, <https://doi.org/10.1016/J.JPOWSOUR.2021.229698>.
144. N. Zhou, K. Prabakaran, B. Lee, et al., "Metal-Free Tetrathienoacene Sensitizers for High-Performance Dye-Sensitized Solar Cells," *Journal of the American Chemical Society* 137 (2015): 4414–4423, <https://doi.org/10.1021/JA513254Z>.
145. A. Das, S. Deshagani, R. Kumar, and M. Deepa, "Bifunctional Photo-Supercapacitor with a New Architecture Converts and Stores Solar Energy as Charge," *ACS Applied Materials & Interfaces* 10 (2018): 35932–35945, <https://doi.org/10.1021/ACSAMI.8B11399>.
146. S. N. J. S. Z. Abidin, S. Mamat, S. A. Rasyid, Z. Zainal, and Y. Sulaiman, "Fabrication of Poly(vinyl Alcohol)-Graphene Quantum Dots Coated with Poly(3,4-Ethylenedioxythiophene) for Supercapacitor," *Journal of Polymer Science Part A: Polymer Chemistry* 56 (2018): 50–58, <https://doi.org/10.1002/POLA.28859>.
147. S. Suriyakumar, P. Bhardwaj, A. N. Grace, and A. M. Stephan, "Role of Polymers in Enhancing the Performance of Electrochemical Supercapacitors: A Review," *Batteries & Supercaps* 4 (2021): 571–584, <https://doi.org/10.1002/BATT.202000272>.
148. K. B. M. Ismail, M. A. Kumar, S. Mahalingam, R. Jayavel, M. Arivanandhan, and J. Kim, "Conducting Polymer Based Electrodes in Metal-Ion Batteries: A State-of-the-Art Review," *Renewable and Sustainable Energy Reviews* 222 (2025): 115982, <https://doi.org/10.1016/J.RSER.2025.115982>.
149. Y. Yin, K. Feng, C. Liu, and S. Fan, "A Polymer Supercapacitor Capable of Self-Charging under Light Illumination," *Journal of Physical Chemistry C* 119 (2015): 8488–8491, <https://doi.org/10.1021/acs.jpcc.5b00655>.
150. Y. Fu, H. Wu, S. Ye, et al., "Integrated Power Fiber for Energy Conversion and Storage," *Energy & Environmental Science* 6 (2013): 805–812, <https://doi.org/10.1039/C3EE23970E>.
151. J. Li, S. Qiu, B. Liu, H. Chen, D. Xiao, and H. Li, "Strong Interaction between Polyaniline and Carbon Fibers for Flexible Supercapacitor Electrode Materials," *Journal of Power Sources* 483 (2021): 229219, <https://doi.org/10.1016/J.JPOWSOUR.2020.229219>.
152. L. L. Chen, X. Bu, W. L. Song, H. S. Chen, W. Wang, and S. Jiao, "Stable Photo-Rechargeable Al Battery for Enhancing Energy Utilization," *Advanced Materials* 36 (2024): 2306701, <https://doi.org/10.1002/ADMA.202306701>.
153. Y. Saito, A. Ogawa, S. Uchida, T. Kubo, and H. Segawa, "Energy-Storable Dye-Sensitized Solar Cells with Interdigitated Nafion/Polypyrrole–Pt Comb-Like Electrodes," *Chemistry Letters* 39 (2010): 488–489, <https://doi.org/10.1246/CL.2010.488>.
154. M. M. Momeni, H. M. Aydisheh, B. K. Lee, and A. Naderi, "Lightweight Flexible Self-Powered Photo-Supercapacitors with Good Stability through Photoelectrochemical Deposition of Tellurium on PPy–V₂O₅ Films as a New Visible Light Active Dual Photoelectrode," *Journal of Materials Chemistry C* 13 (2024): 430–444, <https://doi.org/10.1039/D4TC03090G>.
155. P. Liu, H. X. Yang, X. P. Ai, G. R. Li, and X. P. Gao, "A Solar Rechargeable Battery Based on Polymeric Charge Storage Electrodes," *Electrochemistry Communications* 16 (2012): 69–72, <https://doi.org/10.1016/J.ELECOM.2011.11.035>.
156. D. Solis-Cortés, E. Navarrete-Astorga, R. Schreiber, et al., "A Solid-State Integrated Photo-Supercapacitor Based on ZnO Nanorod Arrays Decorated with Ag₂S Quantum Dots as the Photoanode and a PEDOT Charge Storage Counter-Electrode," *RSC Advances* 10 (2020): 5712–5721, <https://doi.org/10.1039/C9RA10635A>.
157. Z. Wang, J. Cheng, H. Huang, and B. Wang, "Flexible Self-Powered Fiber-Shaped Photocapacitors with Ultralong Cyclife and Total Energy Efficiency of 5.1%," *Energy Storage Materials* 24 (2020): 255–264, <https://doi.org/10.1016/J.ENSMS.2019.08.011>.
158. W. Y. Jin, M. M. Ovhall, H. B. Lee, B. Tyagi, and J. W. Kang, "Scalable, All-Printed Photocapacitor Fibers and Modules Based on Metal-Embedded Flexible Transparent Conductive Electrodes for Self-Charging Wearable Applications," *Advanced Energy Materials* 11 (2021): 2003509, <https://doi.org/10.1002/AENM.202003509>.
159. J. Wang, Y. Ochiai, N. Wu, et al., "Intrinsically Stretchable Organic Photovoltaics by Redistributing Strain to PEDOT: PSS with Enhanced Stretchability and Interfacial Adhesion," *Nature Communications* 15 (2024): 1–12, <https://doi.org/10.1038/S41467-024-49352-4>.
160. J. Li, D. Mo, J. Hu, et al., "PEDOT: PSS-Based Bioelectronics for Brain Monitoring and Modulation," *Microsystems & Nanoengineering* 11 (2025): 1–28, <https://doi.org/10.1038/S41378-025-00948-W>.
161. R. Mulla, "What's New in PEDOT: PSS Thermoelectrics?," *Chemical Communications* 61 (2025): 10878–10897, <https://doi.org/10.1039/D5CC02163D>.
162. Q. Abbas, P. Ratajczak, P. Babuchowska, et al., "Strategies to Improve the Performance of Carbon/Carbon Capacitors in Salt Aqueous Electrolytes," *Journal of the Electrochemical Society* 162 (2015): A5148, <https://doi.org/10.1149/2.0241505JES>.
163. M. Mohsen Momeni, H. Mohammadzadeh Aydisheh, and B. K. Lee, "Effectiveness of MnO₂ and V₂O₅ Deposition on Light Fostered Supercapacitor Performance of WTiO₂ Nanotube: Novel Electrodes for Photo-Assisted Supercapacitors," *Chemical Engineering Journal* 450 (2022): 137941, <https://doi.org/10.1016/J.CEJ.2022.137941>.
164. A. J. Nozik and J. Miller, "Introduction to Solar Photon Conversion," *Chemical Reviews* 110 (2010): 6443–6445, <https://doi.org/10.1021/CR1003419>.
165. T. Trupke, M. A. Green, and P. Würfel, "Improving Solar Cell Efficiencies by Down-Conversion of High-Energy Photons," *Journal of Applied Physics* 92 (2002): 1668–1674, <https://doi.org/10.1063/1.1492021>.
166. A. M. Oni, A. S. M. Mohsin, M. M. Rahman, and M. B. Hossain Bhuiyan, "A Comprehensive Evaluation of Solar Cell Technologies, Associated Loss Mechanisms, and Efficiency Enhancement Strategies for Photovoltaic Cells," *Energy Reports* 11 (2024): 3345–3366, <https://doi.org/10.1016/J.EGYR.2024.03.007>.
167. S. Zhang and N. Pan, "Supercapacitors Performance Evaluation," *Advanced Energy Materials* 5 (2015): 1401401, <https://doi.org/10.1002/AENM.201401401>.
168. P. M. Stanley, F. Sixt, and J. Warnan, "Decoupled Solar Energy Storage and Dark Photocatalysis in a 3D Metal–Organic Framework," *Advanced Materials* 35 (2023): 2207280, <https://doi.org/10.1002/ADMA.202207280>.
169. Y. Pan, J. Wang, S. Chen, et al., "Linker Engineering in Metal–organic Frameworks for Dark Photocatalysis," *Chemical Science* 13 (2022): 6696–6703, <https://doi.org/10.1039/D1SC06785K>.
170. W. Jeong, H. Lee, Y. J. Hwang, et al., "Solution Processing for Colloidal Nanoparticle Thin Film: From Fundamentals to Applications," *Advances in Colloid and Interface Science* 342 (2025): 103538, <https://doi.org/10.1016/J.CIS.2025.103538>.
171. C. Shen, Z. Yin, F. Collins, and N. Pinna, "Atomic Layer Deposition of Metal Oxides and Chalcogenides for High Performance Transistors," *Advanced Science* 9 (2022): 2104599, <https://doi.org/10.1002/ADVS.202104599>.

172. K. Sambath Kumar, D. Pandey, R. Gurjar, and J. Thomas, "Wearable Supercapacitors," *Energy Systems in Electrical Engineering Part F* 2140 (2022): 285–325, https://doi.org/10.1007/978-981-19-4526-7_10.
173. D. Karnaushenko, B. Ibarlucea, S. Lee, et al., "Light Weight and Flexible High-Performance Diagnostic Platform," *Advanced Healthcare Materials* 4 (2015): 1517–1525, <https://doi.org/10.1002/ADHM.201500128>.
174. V. Kumaravel, J. Bartlett, and S. C. Pillai, "Solid Electrolytes for High-Temperature Stable Batteries and Supercapacitors," *Advanced Energy Materials* 11 (2021): 2002869, <https://doi.org/10.1002/AENM.202002869>.